International Journal for Parasitology: Parasites and Wildlife 25 (2024) 100994

Contents lists available at ScienceDirect

International Journal for Parasitology: Parasites and Wildlife

journal homepage: www.elsevier.com/locate/ijppaw

Characterization of four novel actinospore types of fish parasitic myxozoans and the occurrence of *Branchiodrilus hortensis* and *Ophidonais serpentina* from fish farms of Hungary

Nadhirah Syafiqah Suhaimi [a,b], Boglárka Sellyei [a], Zsolt Udvari [c,d], Csaba Székely [a,*], Gábor Cech [a]

[a] HUN-REN Veterinary Medical Research Institute, Budapest, Hungary
[b] Doctoral School of Animal Biotechnology and Animal Science, Hungarian University of Agriculture and Life Sciences, Gödöllő, Hungary
[c] Doctoral School of Biological Sciences, Hungarian University of Agriculture and Life Sciences, Gödöllő, Hungary
[d] Ráckeve Danube Arm Fishing Association, Ráckeve, Hungary

ARTICLE INFO

Keywords:
Myxozoa
Actinospore stages
Morphometric study
Molecular analysis
Fish pond
Hungary

ABSTRACT

Six distinct actinospore types were identified in the intestinal epithelium of oligochaetes collected from the Szigetbecse and Makád fish farms of Ráckeve Danube Arm Fishing Association, in Hungary. Four new types: triactinomyxon type, raabeia type, aurantiactinomyxon type 1, and aurantiactinomyxon type 2, were described morphologically and molecularly from three invertebrate host species: *Limnodrilus hoffmeisteri*, *Ophidonais serpentina,* and *Tubifex tubifex*. The 18S ribosomal DNA (rDNA) analysis revealed that these new types of actinospores did not match any myxospore sequences available in GenBank. Phylogenetic analysis placed the triactinomyxon type within the *Myxobolus* clade that parasitizes cyprinid fish, while the raabeia type and aurantiactinomyxon type 2 were both placed within the *Myxobolus* clade associated with Perciformes fish. Aurantiactinomyxon type 1 was clustered in a clade containing gill-infecting *Henneguya* spp. from Esociformes fish. However, no myxospores have been found yet to link to the newly sequenced actinospores reported in this survey. This study also reports the first occurrence of two oligochaetes species, *Branchiodrilus hortensis* and *Ophidonais serpentina* in Hungary, specifically in fish farms of Ráckeve Danube Arm Fishing Association. Moreover, this is the first report on the involvement of *Ophidonais serpentina* in the life cycle of myxozoans.

1. Introduction

Myxozoa is a group of spore-forming parasites within the phylum Cnidaria that have gathered significant attention from scientists due to their complex life cycle and potential impact on fish health. The life cycle of myxozoans consists of alternation between a vertebrate host (releasing myxospores) and an invertebrate host (releasing actinospores), where actinospores serve as the infective stage for vertebrate, capable of penetrating and infecting the vertebrate host. These spores infect fish and a wide range of aquatic organisms, including amphibians, reptiles, mammals (Dyková et al., 2007; Prunescu et al., 2007) and birds (Bartholomew et al., 2008). Nevertheless, direct transmission of fish-to-fish and annelid-to-annelid can be assumed not possible (Okamura et al., 2015).

In Hungary, actinosporean fauna in oligochaetes is less documented, than myxosporean infections in fish; eight types of actinospores (aurantiactinomyxon, guyenotia, neoactinomyxum, raabeia, triactinomyxon, hungactinomyxon, echinactinomyxon and synactinomyxon) have been described (El-Mansy and Molnár, 1997a, b; El-Mansy and Molnár, 1997a, b; El-Mansy et al., 1998a, b, c; Székely et al., 1998, 1999, 2002, 2005, 2009, 2014; Molnár et al., 1999; Eszterbauer et al., 2000, 2006; Rácz et al., 2004, 2005; Marton and Eszterbauer, 2011; Borkhanuddin et al., 2014; Zhao et al., 2016; Borzák et al., 2021). Surveys of actinosporean infections have been focused in wild environments, including Lake Balaton, which consists of Kis-Balaton Reservoir, Keszthely, Tihany, Balatonvilágos, Balatonszemes, Siófok and the River Zala, as well as the River Tisza. However, surveys on actinosporean fauna in fish farms have only been conducted at the Warmwater Fish Hatchery (TEHAG) in Százhalombatta (El-Mansy et al., 1998b; Rácz et al., 2005; Eszterbauer et al., 2006;

* Corresponding author. HUN-REN Veterinary Medical Research Institute, 1143. Budapest, Hungária krt. 21., Hungary.
E-mail address: szekely.csaba@vmri.hun-ren.hu (C. Székely).

https://doi.org/10.1016/j.ijppaw.2024.100994
Received 14 August 2024; Received in revised form 17 September 2024; Accepted 17 September 2024
Available online 18 September 2024

Marton and Eszterbauer, 2011). In this study, we extend our survey to a new location, fish farms of Ráckeve Danube Arm Fishing Association, to better understand the ecology, distribution, and host preferences of actinospores.

Most myxozoan parasites do not cause visual signs and symptoms in fish hosts, but some species have been identified to cause emerging diseases that impact both wild populations and cultivated fish stocks, leading to substantial economic losses in fisheries and aquaculture industries (Okamura et al., 2015). The prevalence of myxozoan infection in ponds is higher due to the high density of fish, where released actinospores from the infected colonizer annelids find vertebrate hosts more easily. In Hungary, several disease-causing myxozoans have been described from farmed fish, including *Myxobolus lentisuturalis* (Suhaimi et al., 2023), *Sphaerospora molnari* (Eszterbauer et al., 2013), *Sphaerospora renicola* (Eszterbauer and Székely, 2004), *Thelohanellus hovorkai* (Székely et al., 1998), and *Thelohanellus nikolskii* (Borzák et al., 2021). Since Hungary produces 76% of its fish production from pond culture, and the aquaculture industry is growing (EUMOFA, 2023), it is important to study potential myxozoan infections for risk assessment and health management. Hence, this study investigated myxozoan infections in annelids from fish farms belonging to the Ráckeve Danube Arm Fishing Association.

2. Materials and methods

2.1. Study area and sample collection

The survey of actinosporean infections of oligochaetes was conducted in fish ponds of Csepel Island, located about 50 km south of Budapest, Hungary. The survey areas comprised the following fish farms: Szigetbecse (Supplementary Fig. S1) and Makád (Supplementary Fig. S2) belonging to the Ráckeve Danube Arm Fishing Association. The Szigetbecse fish farm consists of 12 small fishponds with a total area of 1.9 ha, while the Makád fish farm consists of 6 fish ponds with 87.35 ha. These fish farms mainly produced carp (*Cyprinus carpio*) but also a small proportion of herbivores and predatory fish such as pike (*Esox lucius*), asp (*Aspius aspius*), pikeperch (*Sander lucioperca*), tench (*Tinca tinca*), wels catfish (*Silurus glanis*), and grass carp (*Ctenopharyngodon idella*) in the amount of approximately 200–220 tons of fish annually. A large portion of this production will be stocked into the Ráckeve Danube Branch to sustain fish populations.

Sediment containing oligochaetes was collected from the ponds of fish farms with low water levels on May 31, 2023, using a shovel and a 1000 μm mesh size net. The collected sediments were transported with minimal pond water to the Fish Pathology and Parasitology Laboratory of the HUN–REN Veterinary Medical Research Institute in Budapest, Hungary. In the laboratory, mud was maintained in the buckets with an aeration system, regularly supplied with dechlorinated tap water to avoid it drying up and kept at a temperature of 23 °C. The oligochaetes were hand-sorted on light panel covered transparent tray and placed individually into the wells of the 48-well microtiter plates containing dechlorinated water. Large-sized oligochaetes, such as *Branchiura sowerbyi* and *Branchiodrilus hortensis* were placed individually into the wells of the 24-well microtiter plates. Each plate was examined daily for 2 months to detect the presence of released actinospores using Zeiss Axiovert 25 inverted microscope (Zeiss, Jena, Germany).

2.2. Microscopic examination

Freshly released actinospores from infected oligochaetes were examined on a glass slide and photographed under the light microscope (Olympus BX53) equipped with Olympus DP74 digital camera. The spores were collected in 1.5 mL of Eppendorf tube and preserved in 80% ethanol for molecular studies. Spore morphology and morphometric parameters were determined from fresh spores following the guidelines of Lom et al. (1997) using ImageJ software (http://imagej.nih.gov/ij). All measurements are given as the mean value and standard deviation (SD) followed by the range of variation in parentheses in micrometres (μm) and number (n) of measured actinospores.

The infected worms were collected, with the anterior part preserved in 80% ethanol to facilitate species identification through molecular techniques. Consequently, the posterior segment was preserved in 5% neutral buffered formalin, embedded in paraffin wax, and sliced into 4–5 μm thick sections. For histological analysis, these sections were stained with haematoxylin and eosin (H&E). The sections were examined with an Olympus BX53 microscope and photographed with an Olympus DP74 digital camera to determine the site of infection within the oligochaetes.

2.3. Molecular analysis

Preserved actinospores in 80% ethanol were centrifuged at 13,000 rpm for 15 min, and the ethanol was removed by pipetting. The pelleted spores were washed twice with elution buffer (10 mM Tris-HCl, pH 8.5) to remove residual ethanol. Genomic DNA extraction was performed from the pellet using the Geneaid Tissue Genomic DNA Mini kit (Geneaid Biotech Ltd., Taiwan) following the manufacturer's recommended protocol for animal tissues. Subsequently, direct PCR was conducted to amplify the 18S rDNA gene of the actinospores using different primer combinations listed in Table 1. The polymerase chain reactions (PCR) were performed in 25 μL reaction volumes, containing 2 μL of template DNA, 1 × of DreamTaq buffer (10 × ; Thermo Scientific), 0.2 mM of dNTP mix (10 mM; Thermo Scientific), 1.25 U of DreamTaq polymerase (5 U; Thermo Scientific), 12.5 pmol of each primer, and molecular water. Different primers' amplifications of PCR reactions were carried out using different protocol conditions. Both ERIB10-Myx1F and ERIB10-MyxospecF were amplified with an initial denaturation at 95 °C for 3 min, followed by 35 cycles of 95 °C for 1 min, different annealing temperatures (55 °C and 50 °C, respectively) for 1 min, 72 °C for 2 min and a final extension at 72 °C for 7 min. Concurrently, PCR reactions of ERIB1-ACT1R were carried out according to Atkinson and Bartholomew (2009). For the identification of oligochaete hosts, 16S rRNA gene of mitochondrial DNA (mtDNA) was amplified using 16sar-L and 16sbr-H primers (Palumbi et al., 2002) in a 25 μL reaction mixture, containing the same amount of components as master mix for actinospores mentioned above. PCR reactions of 16S rRNA were conducted using the conditions previously described by Rocha et al. (2019a). PCR products were visualized by agarose gel electrophoresis on 1% TAE gel stained with ethidium bromide. The PCR products of the expected size were purified using DNA Fragment Purification kit (InViTek GmbH, Berlin, Germany) and sequenced bidirectionally using the BigDye Terminator v3.1 Cycle Sequencing Kit (Applied Biosystems, Foster City, CA, USA) and an ABI PRISM 3100 Genetic Analyser (Applied Biosystems) with primers listed in Table 1.

2.4. Sequence assembly

The partial 18S rDNA sequences obtained from actinospores originating from infected oligochaete were assembled and checked using Geneious Prime v.11.1 (Kearse et al., 2012). Five newly obtained 18S rDNA sequences and 27 closely related published sequences were retrieved from GenBank database, and *Chloromyxum cyprini* (AY604198) was chosen as an outgroup to assess the phylogenetic analysis. The nucleotide sequences were aligned using the Clustal W algorithm (Thompson et al., 1994) in MEGA X (Kumar et al., 2018). The phylogenetic tree was obtained using Maximum Likelihood (ML) analysis. Gaps were treated with the option of partial deletion and with 75% site coverage cutoff. ML analysis was calculated using GTR + G + I model according to the model selection by Akaike information criterion (AIC), with bootstrap confidence values calculated with 1000 replications. The resulting topologies were visualized in MEGA X (Kumar et al., 2018) and annotated with Inkscape (Free Software Foundation, Inc., MA, USA).

Table 1
List of primers used for DNA amplification and sequencing of each actinospore type and oligochaete.

Specimen	Primer	Application	Reference
Triactinomyxon type	ERIB10	PCR and sequencing	Barta et al. (1997)
	MyxospecF	PCR and sequencing	Fiala (2006)
	Myxgen4F	Sequencing	Diamant et al. (2004)
	ACT1R	Sequencing	Hallett and Diamant (2001)
Raabeia type	ERIB10	PCR and sequencing	Barta et al. (1997)
	Myx1F	PCR	Hallett and Diamant (2001)
	ERIB1	PCR	Barta et al. (1997)
	ACT1R	PCR and sequencing	Hallett and Diamant (2001)
	ACT1fr	Sequencing	Hallett and Diamant (2001)
	18E	Sequencing	Hillis and Dixon (1991)
	Myxgen4F	Sequencing	Diamant et al. (2004)
Aurantiactinomyxon type 1	ERIB10	PCR and sequencing	Barta et al. (1997)
	Myx1F	PCR and sequencing	Hallett and Diamant (2001)
	ERIB1	PCR and sequencing	Barta et al. (1997)
	ACT1R	PCR and sequencing	Hallett and Diamant (2001)
	ACT3F	Sequencing	Hallett and Diamant (2001)
	Myxgen4F	Sequencing	Diamant et al. (2004)
Aurantiactinomyxon type 2	ERIB10	PCR	Barta et al. (1997)
	Myx1f	PCR	Hallett and Diamant (2001)
	ERIB1	PCR and sequencing	Barta et al. (1997)
	ACT1R	PCR and sequencing	Hallett and Diamant (2001)
	SphR	Sequencing	Eszterbauer and Székely (2004)
	ACT1fr	Sequencing	Hallett and Diamant (2001)
	ACT3F	Sequencing	Hallett and Diamant (2001)
Oligochaete	16sar-L	PCR and sequencing	Palumbi et al. (2002)
	16sbr-H	PCR and sequencing	Palumbi et al. (2002)

The distance estimation was performed using a distance matrix model *p*-distance for transitions and transversions in MEGA X software package.

3. Results

During a seven-month follow-up period, a total of 1920 oligochaetes were isolated from sediment collected from fish farms at Szigetbecse and Makád, with 1680 from fish ponds of Szigetbecse and 240 from fish ponds of Makád. Actinosporean infection was detected in the intestinal epithelium of 22 oligochaetes, resulting in an overall prevalence of 1.14% (22 out of 1920 oligochaetes examined) in the fish farms of Ráckeve Danube Arm Fishing Association. The prevalence of infection varied according to the sampling site, being highest in the fish ponds at Szigetbecse (1.25%), with 21 infected out of 1680 oligochaetes examined, and 0.42% in the fish ponds at Makád, with only one infected out of 240 oligochaetes examined. In total, six different actinospore types belonging to collective groups of triactinomyxon, raabeia, and aurantiactinomyxon were identified in this study. Two out of six types were identified as triactinomyxon of *Myxobolus pseudodispar* previously described by Forró and Eszterbauer (2016) (KU340985) and raabeia type 1 by Borkhanuddin et al. (2014) (KJ152184). Others were identified as new types comprising one triactinomyxon, one raabeia and two aurantiactinomyxon and described here based on morphological (Table 2) and molecular characterization. The nucleotide sequences of actinospore were 1559, 1648, 1917 and 2019 bps long. The alignment of the sequences contained 2151 nucleotide positions including 950 conservative and 1148 variable nucleotide sites.

This survey revealed the presence of eight morphologically distinct species of oligochaetes in the sediment samples: *Branchiura sowerbyi*, *Tubifex tubifex*, *Limnodrilus hoffmeisteri*, *Dero* sp., *Stylaria* sp., *Potamothrix* sp., *Branchiodrilus hortensis,* and *Ophidonais serpentina*. However, myxozoan infections were detected only in three genera: *Limnodrilus*, *Tubifex,* and *Ophidonais*, with worms belonging to *Limnodrilus* comprising 32% of oligochaetes examined. The oligochaete hosts were morphologically identified following the characteristics described by Timm (2009) and through nucleotide analysis of the mitochondrial 16S rRNA gene (Rocha et al., 2019a). A BLAST search of the 16S rRNA sequences obtained from the infected oligochaetes revealed a 99.4% similarity to the sequences of *Ophidonais serpentina* (DQ459939) and *Tubifex tubifex* (JQ247495), as well as a 99.1% similarity to *Limnodrilus hoffmeisteri* (KY369377). Therefore, it is confirmed that the infected worms belong to *Ophidonais serpentina*, *Tubifex tubifex*, and *Limnodrilus hoffmeisteri*.

Noteworthy, we discovered *B. hortensis* and *O. serpentina* in the sediment sample, marking their first detection in Hungary, specifically in fish ponds of Ráckeve Danube Arm Fishing Association, where the water source originated from Danube River (Ráckeve Danube Branch). The morphological characteristics of the examined individuals corresponded to the species *B. hortensis* according to the guides by Nesemann et al. (2004), Timm (2009), and van Haaren and Soors (2013). This species can be recognized by having pairs of dorso-lateral gills nearly along the body (Fig. 1A). On the anterior part of the body, simple pointed and fine needle setae are enclosed within the gill (Fig. 1B). In contrast, the needle setae are free and not enclosed within the gills on the posterior part of the body (Fig. 1C). Furthermore, 4–5 setae per bundle can be seen on the ventral part of the body (Fig. 1D). *Ophidonais serpentina* in this study can be characterised by having a pale body with pigment stripes on its anterior segments (Fig. 2A), and the presence of eye spots (Fig. 2B), which are similar to characteristics described by Yu et al. (2022). The needle setae are absent at posterior segments (Figs. 2C), and 3–5 setae per bundle can be seen at the ventral part of the body (Fig. 2D). Molecular analyses confirmed that the 16S rRNA sequences showed 99.1% similarity to the sequence of *Branchiodrilus hortensis* (KY333141), and 99.4% similarity to *Ophidonais serpentina* (DQ459939), respectively. Hence, it is confirmed by both morphological and molecular analyses that the oligochaetes belong to *B. hortensis* and *O. serpentina.*

3.1. Description of novel actinospore types

3.1.1. Triactinomyxon type (Fig. 3A and B)

Description: Spore body: cylindrical, elongated, 37.6 ± 4.9 (29.1–48.8) μm long, 13.6 ± 1.4 (11.5–15.8) μm wide. Style: long, 131.2 ± 13.9 (103.6–154.4) μm long, 16.4 ± 1.1 (14.7–19.6) μm wide. Total length: 172.4 ± 10.6 (153.3–192.4) μm. Caudal process: upward, tapering to pointed ends, equal length, 274.89 ± 15.3 (257.8–298.9) μm long, 21.2 ± 1.9 (17.2–24.4) μm wide at base. Largest span: 486.2 ± 76.3 (311.2–560.3) μm. Valve cell nuclei: located at base of caudal processes, 4.9 ± 0.7 (4.1–6.1) μm diameter (n = 5). Polar capsule: pyriform, equal size, protruding from anterior end, 6.0 ± 0.9 (4.3–7.7) μm long, 4.0 ± 0.6 (3.2–5.0) μm wide. Polar tubule: coiled 4–5 times. Sporoplasm: 32 secondary cells. Measurements from 15 fresh actinospores.

Table 2
Measurements (mean value and standard deviation (SD) followed by the range of variation in parentheses) of freshly released actinospores from oligochaetes. L: length, W: width, D: diameter. All measurements are in μm.

Actinosporean	Caudal processes		Spore body		Polar capsule		Style		No. of secondary cell
	L	W	L	W	L	W	L	W	
Triactinomyxon type 1	274.8 ± 15.3 (257.8–298.9)	21.2 ± 1.9 (17.2–24.4)	37.6 ± 4.9 (29.1–48.8)	13.6 ± 1.4 (11.5–5.8)	6.3 ± 0.7 (4.7–7.6)	4.0 ± 0.4 (3.4–5.0)	131.2 ± 13.9 (103.6–154.4)	16.4 ± 1.1 (14.7–19.6)	32
Raabiea type 1	153.0 ± 16.5 (123.9–136.0)	7.0 ± 0.9 (5.5–8.7)	51.8 ± 2.7 (47.7–50.2)	5.5 ± 0.9 (4.1–6.0)	5.0 ± 0.8 (3.9–4.7)	2.8 ± 0.4 (1.9–2.7)	Absent	Absent	16
Aurantiactinomyxon type 1	25.7 ± 2.9 (21.3–31.6)	7.4 ± 1.3 (4.2–10.1)	D: 13.6 ± 1.9 (8.2–17.3)		D: 2.4 ± 0.3 (1.9–3.3)		Absent	Absent	32
Aurantiactinomyxon type 2	64.5 ± 4.2 (55.8–71.6)	4.7 ± 0.6 (3.7–5.7)	D: 10.5 ± 0.9 (8.8–13.3)		D: 2.6 ± 0.3 (2.0–3.2)		Absent	Absent	16

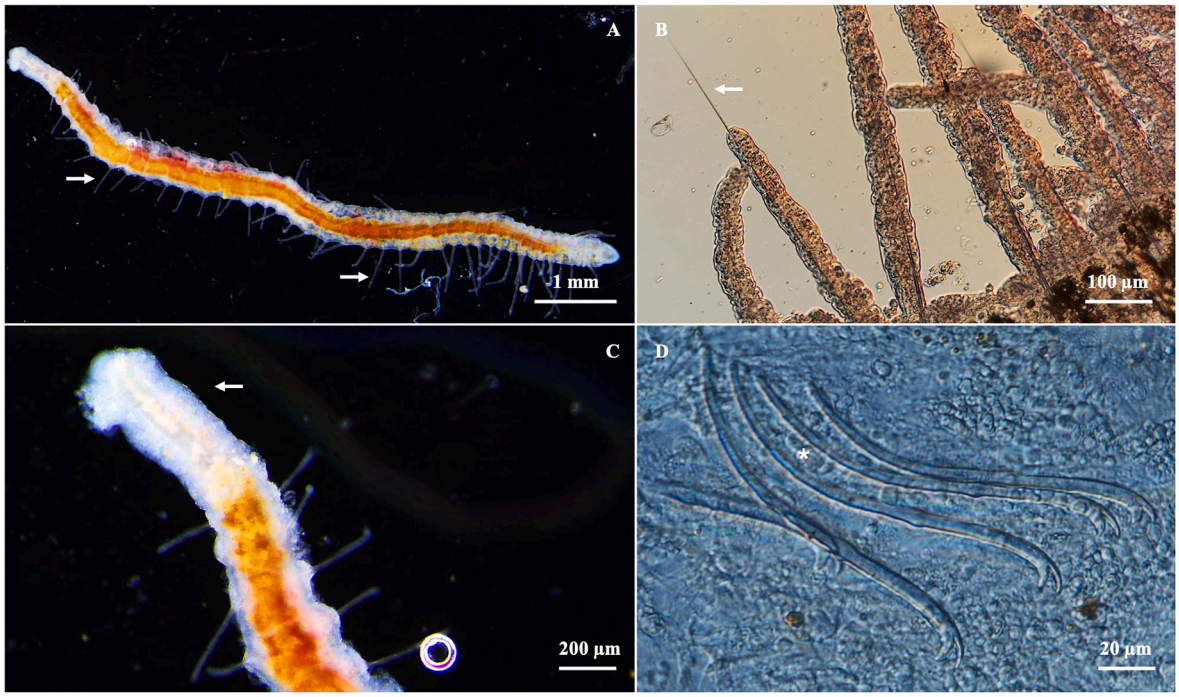

Fig. 1. *Branchiodrilus hortensis*. A) Dorso-lateral gills present along the entire length of the body. B) Simple, fine, pointed needles located at the anterior of the body. C) Posterior part of the body. D) 4–5 hair setae located on the ventral part of the body.

Host: Limnodrilus hoffmeisteri Claparède, 1862.
Site of infection: The intestinal epithelium.
Prevalence: 0.14% (1 out of 735 infected host species).
Locality: Szigetbecse, Csepel Island, Hungary.
Type *material*: Series of phototypes was deposited in the collection of Fish Pathology and Parasitology Research Team, Veterinary Medical Research Institute, Budapest, Hungary.
18S rDNA sequence: One sequence with a length of 1648 bp was deposited in GenBank under the accession number PQ164813.

Remarks. The morphology and morphometrics of the present triactinomyxon type were distinct from those described in the literature. Triactinomyxon type of the present study was morphologically similar to triactinomyxon type 2 (Székely et al., 2014) but was not the same morphometrically. The spore body length of the triactinomyxon type in this study closely resembled those of triactinomyxon type 5 (El-Mansy et al., 1998a) and triactinomyxon type 3 (Lowers and Bartholomew, 2003). The triactinomyxon type examined also greatly resembled to triactinomyxon type 4 described by El-Mansy et al. (1998a), though the polar capsules in our study were slightly smaller (6.0 × 4.0 vs 5.9 × 3.5). Additionally, the length of the style of the triactinomyxon type in present study was also slightly smaller compared to triactinomyxon type 4 of El-Mansy et al. (1998b). Notably, the length and width of the caudal processes of the triactinomyxon type differed from those described in the literature. The 18S rDNA sequence from the triactinomyxon type did not match any of the myxozoan sequences available in GenBank and was most similar to those within the clade of cypriniform-infecting myxobolids (Fig. 8). Distance estimation of the newly obtained sequence showed the highest similarities to *Myxobolus diversicapsularis* reported from the gills of *Rutilus rutilus* (98.4%; GU968199) and triactinomyxon sp. type 3 (98.0%; AY495706). Other sequences (AY495705, MK053784, AY495707, DQ439807, FJ851449) presented percentage similarity values lower than 98.0% (Supplementary Table S1). Phylogenetic analysis revealed that the triactinomyxon type clustered with *M. diversicapsularis* and triactinomyxon type 3, with high bootstrap support. Additionally, the triactinomyxon type identified in this study formed a sister group with two species of *Myxobolus* and triactinomyxon type 2. This triactinomyxon type was also positioned basally in a monophyletic clade together with triactinomyxon type 4, *Myxobolus rotundus*, *Myxobolus diversipsularis*, triactinomyxon type 3, *Myxobolus arcasii*, triactinomyxon type 2 and *Myxobolus muellericus*, with maximum bootstrap support (Fig. 8).

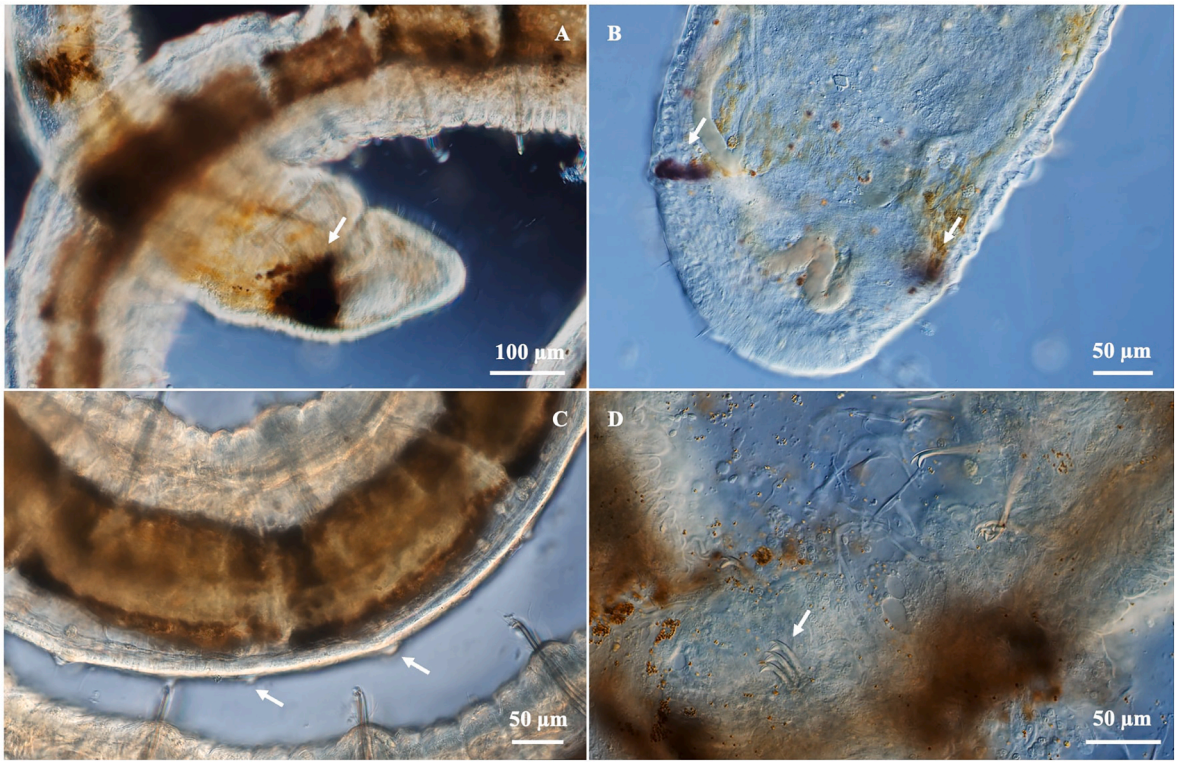

Fig. 2. *Ophidonais serpentina*. A) Pigment stripes at the anterior part of the body. B) Eye spots present. C) Needle setae absent at the posterior part of the body. D) 3–5 setae located on the ventral part of the body.

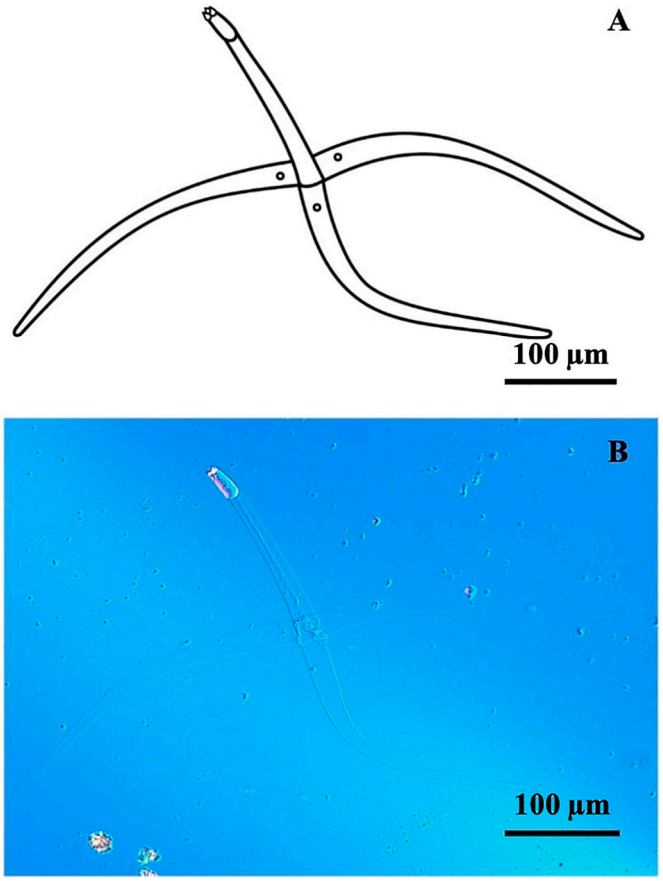

Fig. 3. Triactinomyxon type. A) Schematic drawing of mature actinospore. B) Fresh unstained triactinomyxon type.

3.1.2. Raabeia type (Fig. 4A–D)

Description: Spore body: elongated, cylindrical in side view, 51.8 ± 2.7 (47.7–50.2) µm long, 5.5 ± 0.9 (4.1–6.0) µm wide. Caudal process: equal length, long, curved upwards, tapering to sharp point, 153.0 ± 16.5 (123.9–136.0) µm long and 7.0 ± 0.9 (5.5–8.7) µm wide at base. Valve cell nuclei: located at spore body base, 3.2 ± 0.6 (2.2–4.6) µm diameter (n = 19). Polar capsule: spherical in apical view, pyriform in side view, protruding from anterior end, 5.0 ± 0.8 (3.9–4.7) µm long and 2.8 ± 0.4 (1.9–2.7) µm wide, each with 4 coils polar tubule. Sporoplasm: 16 secondary cells, arranged in 2 columns. Measurements from 30 fresh actinospores.

Host: Limnodrilus hoffmeisteri Claparède, 1862.

Site of infection*:* The intestinal epithelium. Pansporocyst of the raabeia type is visible in the intestinal epithelium of the infected oligochaete (Fig. 4E).

Prevalence: 1.63% (12 out of 735 infected host species).

Locality: Szigetbecse, Csepel Island, Hungary.

Type material*:* Series of phototypes was deposited in the collection of Fish Pathology and Parasitology Research Team, Veterinary Medical Research Institute, Budapest, Hungary.

18S rDNA sequence: One sequence with a length of 2019 bp was deposited in GenBank under the accession number PQ217959.

Remarks. Morphology of the raabeia type resembled raabeia type 2 (Borkhanuddin et al., 2014) and "triactinomyxon 'F'" (Xiao and Desser 1998), with both having cylindrical spore body and 16 secondary cells arranged in 2 columns. This morphology did not resemble any of the raabeia types described so far. In terms of morphometric measurements, the raabeia type of present study was most similar to "triactinomyxon 'F'" in polar capsule length, although "triactinomyxon 'F'" has larger caudal processes and a slightly smaller spore body. Compared to the raabeia type of Borkhanuddin et al. (2014), our raabeia type had slightly larger caudal processes but a smaller spore body. Additionally, the spore body length of our raabeia type closely resembled Raabeia magna (Janiszewska, 1957), while the width was most similar to raabeia type 2

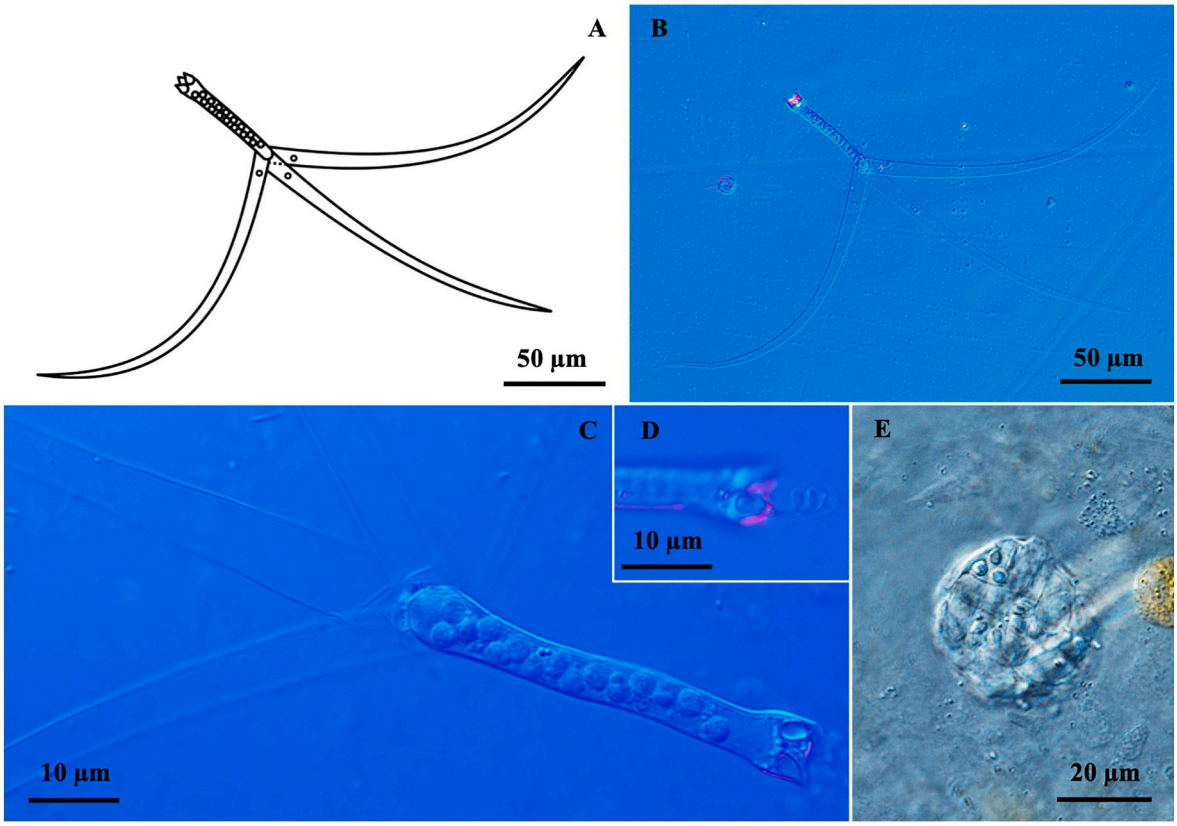

Fig. 4. Raabeia type. A) Schematic drawing of mature actinospore. B) Fresh unstained raabeia type. C) Higher magnification of spore body showing two of three polar capsules and secondary cells arranged in two columns. D) Polar capsule contains 4 coils. E) Pansporocyst of the raabeia type in the intestinal epithelium of an infected oligochaete.

(Borkhanuddin et al., 2014). The length of the caudal processes of the raabeia type was slightly larger than the raabeia type of Rosser et al. (2014) but slightly narrower. However, the spore body width was similar to raabeia type 2 of Borkhanuddin et al. (2014). The polar capsule length was similar to Raabeia furciligera (Marques, 1984) and raabeia type 2 of Oumouna et al. (2003). The 18S rDNA sequence from the raabeia type did not match any of the myxozoan sequences available in GenBank. Distance estimation of the newly obtained sequence showed the highest similarity to "triactinomyxon 'F'" (98.7%; AF378351). Other sequences (U13828, MW588907, JN896706, KJ152184, MK592012), presented percentage similarity values lower than 98.0% (Supplementary Table S1). Phylogenetic analysis revealed that the raabeia type clustered with "triactinomyxon 'F'", with maximum bootstrap support, and formed a sister group with raabeia type 1, *Myxobolus dechtiari*, and *Myxobolus* sp. (Fig. 8).

3.1.3. *Aurantiactinomyxon type 1 (Fig. 5A–E)*

Description: Spore body: triangular apical view, 13.6 ± 1.9 (8.2–17.3) µm diameter, subspherical in side view. Caudal process: three leaf-like, equal size, 25.7 ± 2.9 (21.3–31.6) µm long and 7.4 ± 1.3 (4.2–10.1) µm wide at base, slightly curved downwards in side view. Valve cell nuclei: located randomly in each caudal process, 2.1 ± 0.3 (1.5–2.6) (n = 15). Polar capsule: positioned at apex of spore body, globular in apical view, 2.4 ± 0.3 (1.9–3.3) µm diameter, pyriform in side view. Polar tubule: not visible. Sporoplasm: approximately 32 secondary cells. Measurements from 20 fresh actinospores.

Host: Ophidonais serpentina (Müller, 2015).

Site of infection: The intestinal epithelium.

Prevalence: 0.9% (1 out of 110 infected host species).

Locality: Makád, Csepel Island, Hungary.

Type material: Series of phototypes was deposited in the collection of Fish Pathology and Parasitology Research Team, Veterinary Medical Research Institute, Budapest, Hungary.

18S rDNA *sequence:* One sequence with a length of 1917 bp was deposited in GenBank under the accession number PQ189140.

Remarks. The morphology and morphometrics of the present aurantiactinomyxon type 1 were inconsistent with any previously described aurantiactinomyxon types. The closest morphology resemblances were found with the aurantiactinomyxon type of Zhao et al. (2017). However, the present aurantiactinomyxon type 1 possessed longer caudal processes and a smaller spore body, although both aurantiactinomyxon types had a similar number of secondary cells. In addition, the morphometric measurements of the present aurantiactinomyxon type 1 were almost similar to the aurantiactinomyxon type described by McGeorge et al. (1997), with the present aurantiactinomyxon type 1 having slightly longer caudal processes and smaller spore body, and polar capsules diameters. The spore body diameter closely resembled that of aurantiactinomyxon type 1 (Székely et al., 2003). The present aurantiactinomyxon type 1 had a slightly larger polar capsule size than aurantiactinomyxon type 1 (El-Mansy et al., 1998a) and aurantiactinomyxon type 9 (El-Mansy et al., 1998b) collected from *Branchiura sowerbyi*, while it was slightly smaller than aurantiactinomyxon type 4 (Özer et al., 2002) from *Tubifex tubifex*. The 18S rDNA sequence from the aurantiactinomyxon type 1 did not match any of the myxozoan sequences available in GenBank and was most similar to those clustered with gill-infecting myxobolids (Fig. 8). Distance estimation of the newly obtained sequence showed the highest similarity to *Henneguya* sp. reported from the gills of *Esox lucius* (96.9%; EU732601). Other sequences (EU732600, MT711164, AF378356, MZ905347, KM000055, DQ673465, MZ905344, KY996557, JF714994, AB693050, OQ269720) presented percentage similarity values lower than 96.0% (Supplementary Table S1). Phylogenetic analysis revealed that the

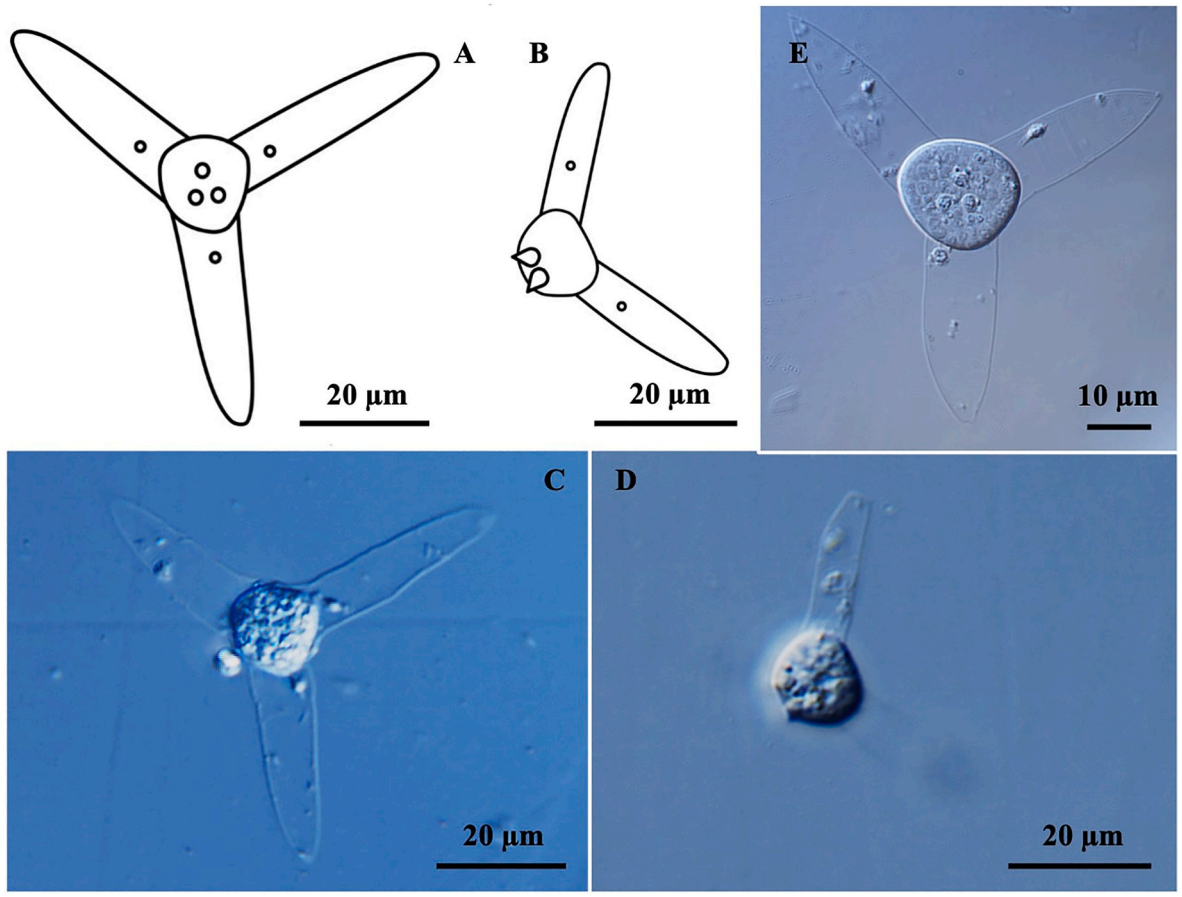

Fig. 5. Aurantiactinomyxon type 1. A) Schematic drawing of mature actinospore in apical view. B) Schematic drawing of side view. Fresh unstained aurantiactinomyxon type 1 in C) apical view and D) side view. E) Higher magnification of mature spore showing the secondary cells in the spore body.

aurantiactinomyxon type 1 clustered with *Henneguya* sp. *Esox lucius* with high bootstrap support. Additionally, the aurantiactinomyxon type 1 identified in this study formed a sister group with *Henneguya lobosa* and *Henneguya michiganensis* with maximum bootstrap support. This aurantiactinomyxon type 1 was also positioned basally in a monophyletic clade together with seven species of *Henneguya*, Aurantiactinomyxon type, and *Myxobolus* sp. (Fig. 8).

3.1.4. *Aurantiactinomyxon type 2 (Fig. 6A–E)*

Description: Spore body: spherical in apical view, 10.5 ± 0.9 (8.8–13.3) µm diameter, bulbous in side view. Caudal process: long, straight, sharp point, equal length, 64.5 ± 4.2 (55.8–71.6) µm long, 4.7 ± 0.6 (3.7–5.7) µm wide at base, slightly curved downwards in side view. Valve cell nuclei: located randomly in each caudal process. Polar capsule: positioned at apex of spore body, globular in apical view, 2.6 ± 0.3 (2.0–3.2) µm diameter, pyriform in side view. Polar tubule: not visible. Sporoplasm: approximately 16 secondary cells. Measurements from 30 fresh actinospores.

Host: Tubifex tubifex (Müller, 2015).

Site of infection: The intestinal epithelium. Histological analysis and microscopic examination showed that the pansporocysts located in the intestinal epithelium of the infected oligochaetes (Fig. 7A–C). In the semithin sections, matured spores could be observed within the pansporocyst (Fig. 7D).

Prevalence: 0.35% (2 out of 573 infected host species).

Locality: Szigetbecse, Csepel Island, Hungary.

Type mat*erial:* Series of phototypes was deposited in the collection of Fish Pathology and Parasitology Research Team, Veterinary Medical Research Institute, Budapest, Hungary.

18S rDNA sequence: Two sequences from different individuals with lengths of 1559 bp and 1582 bp were deposited in the GenBank under the accession numbers PQ189138 and PQ189141, respectively.

Remarks. The morphology and morphometrics of the present aurantiactinomyxon type 2 were inconsistent with any previously described aurantiactinomyxon types. The spore body diameter of the aurantiactinomyxon type 2 closely resembled those described by Borkhanuddin (2013), Borzák et al. (2021), and Freeman and Kristmundsson (2018), with the present aurantiactinomyxon type 2 having a larger spore body. Notably, the length and width of the caudal processes of the aurantiactinomyxon type 2 differed from those described in the literature, with the present aurantiactinomyxon type 2 having larger caudal processes than previously described aurantiactinomyxon types but smaller than those described by El-Mansy et al. (1998b). Additionally, the diameter of polar capsules was closest similar to those of aurantiactinomyxon type 1 (Özer et al., 2002), aurantiactinomyxon type B (Eszterbauer et al., 2006) and aurantiactinomyxon types described by Borkhanuddin (2013), Rocha et al. (2019b), Borzák et al. (2021). Two almost identical 18S rDNA sequences (99.6%) from the aurantiactinomyxon type 2 did not match any of the myxozoan sequences available in GenBank. Distance estimation of the newly obtained sequences showed the highest similarities to *Myxobolus* sp. (89.1%, 88.5%; U13828), the raabeia type identified in this study (88.6%, 87.9%; PQ217959), *Myxobolus dechtiari* (87.1%, 86.7%, MW588907), and the "triactinomyxon 'F'" (87.0%, 87.7%; AF378351). Other sequences (JN896706, KJ152184, MK592012) presented percentage similarity values lower than 85.0% (Supplementary Table S1). Phylogenetic analysis revealed that the aurantiactinomyxon type 2 formed a well-supported sister group with the *Myxobolus* spp. clade, including *Myxobolus inornatus*, *Myxobolus doubleae*, *Myxobolus* sp., and *Myxobolus*

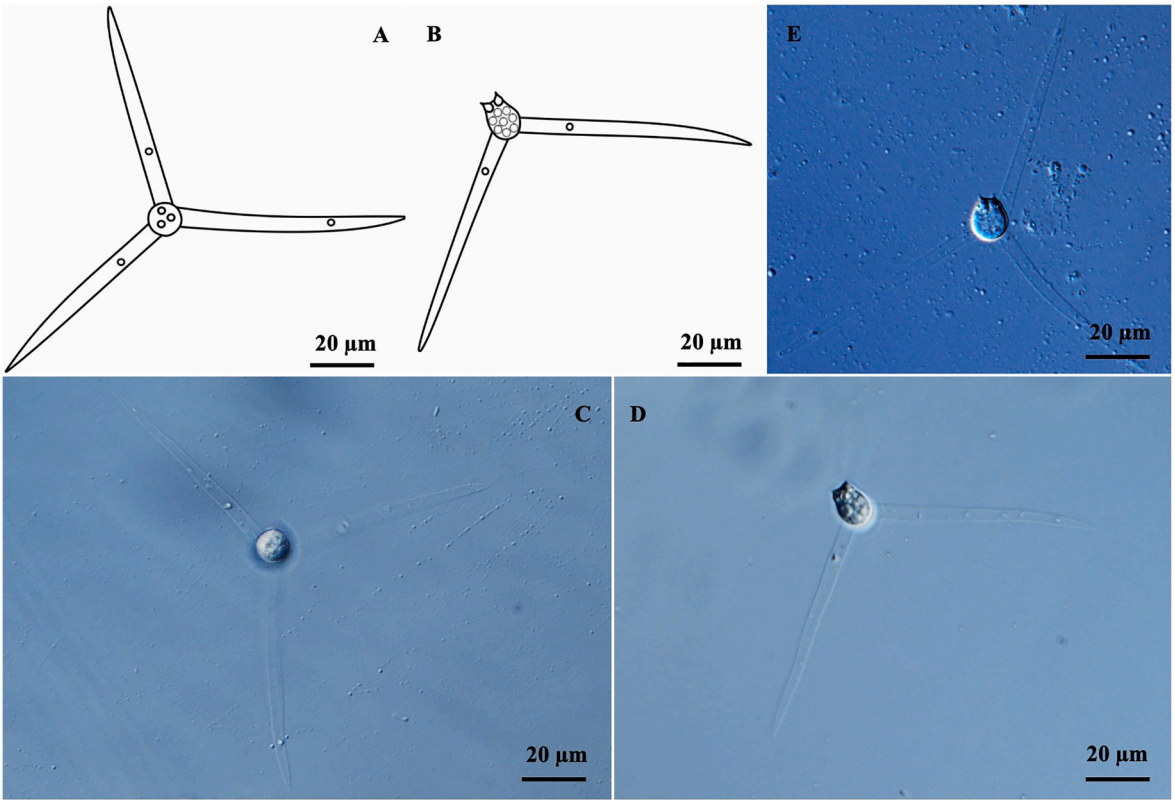

Fig. 6. Aurantiactinomyxon type 2. A) Schematic drawing of mature actinospore in apical view. B) Schematic drawing of side view. Fresh unstained aurantiactinomyxon type 2 in C) apical view and D) side view. E) Mature spore in side view showing three caudal processes.

dechtiari, as well as triactinomyxon F, raabeia type 1 and raabeia type identified in the present study (Fig. 8).

4. Discussion

In the past, studies on actinospores in fish ponds in Hungary were conducted and well-studied only at the TEHAG fish farm, describing more than 30 actinospore types from six collective groups, including triactinomyxon, raabeia, neoactinomyxum, aurantiactinomyxon, hungactinomyxon, echinactinomyxon, (El-Mansy et al., 1998b; Rácz et al., 2005; Eszterbauer et al., 2006; Marton and Eszterbauer, 2011). In this study, we attempted to explore new fish farm locations in Hungary to survey myxozoan diversity and describe new actinospore stages of myxozoans and their alternate annelid hosts. During a seven-month follow-up period, we successfully described novel four actinospore types namely raabeia, triactinomyxon, and aurantiactinomyxon from 1920 examined oligochaetes collected from Szigetbecse and Makád fish farms located in Csepel Island. We also successfully detected the occurrence of two oligochaetes species in Hungary for the first time.

In Hungary, several species of oligochaetes are commonly found in natural waters and fish ponds, such as *Branchuira sowerbyi, Limnodrilus hoffmeisteri, Tubifex tubifex, Isochaetides michaelseni, Nais* sp., *Stylaria* sp., and *Dero* sp. (El-Mansy et al., 1998a, b; Borkhanuddin et al., 2014; Székely et al., 2014; Atanacković et al., 2020). However, *Branchiodrilus hortensis* and *Ophidonais serpentina* have never been recorded in Hungary until our discovery at the fish farms of Ráckeve Danube Arm Fishing Association. *Branchiodrilus hortensis* is native in Asia (India, Pakistan, Burma, China, Japan, Russian Far East, Indonesia), Australia and Africa (Ghana, Sudan, Zambia) and rarely found in Europe (Cekanovskay, 1962; Brinkhurst and Jamieson, 1971). So far, *B. hortensis* has been recorded in the U.K., the Netherlands, Belgium, France, Slovakia, Germany, and recently in Serbia (van Haaren et al., 2005; Šporka, 2009; van Haaren and Soors, 2013; Martin et al., 2018; Baumgartner et al., 2020; Atanacković et al., 2021). Contrarily, *O. serpentina* is a common species in Europe (Slovakia, Poland, Turkey), America, and Africa (Spenser and Wisseman, 1993; Krno et al., 1999; Arslan and Şahin, 2006; George et al., 2009; Krodkiewska et al., 2016). The occurrence of both *B. hortensis* and *O. serpentina* in Hungary, specifically in fish ponds of Ráckeve Danube Arm Fishing Association, can be attributed to the water source coming from Danube River (Ráckeve Danube Branch). This is supported by the presence of both *B. hortensis* and *O. serpentina* populations in Danube River of Slovakia and *B. hortensis* population in Serbia (Šporka, 2009; Atanacković et al., 2021), indicating their spread through Danube River into Hungary. Danube River traversing 10 European countries, provides a hydrological connectivity that allows for the dispersal of *B. hortensis* and *O. serpentina* through water flow and river currents into Hungarian waters. Furthermore, the fish farms of Ráckeve Danube Arm Fishing Association source water come from Danube River (Ráckeve Danube Branch) and are directly connected to the river's ecosystem. This connection enables the introduction of the riverine species into the controlled environments of fish farms. As the water is pumped or flows into the farms, it brings with it the organisms of the river, including *B. hortensis* and *O. serpentina*.

The prevalence of infected worms in this study was low (1.14%). These results contrast with the findings of El-Mansy et al. (1998b), Özer et al. (2002), and Eszterbauer et al. (2006), who reported a high prevalence of infection in oligochaetes collected from fish farms in Hungary and an Atlantic salmon fish farm in Scotland. For example, El-Mansy et al. (1998b) determined a 3.14% prevalence rate during a year-long examination with biweekly sampling, while Özer et al. (2002) detected a total prevalence of 2.9% over two years of oligochaete examination and Eszterbauer et al. (2006) reported a prevalence rate of 1.82% during an eight-month examination of oligochaetes with sampling conducted twice. Here, the lower prevalence could be explained by the sampling strategy, where oligochaetes were collected once and studied in a seven-month follow-up period, compared to a longer sampling duration

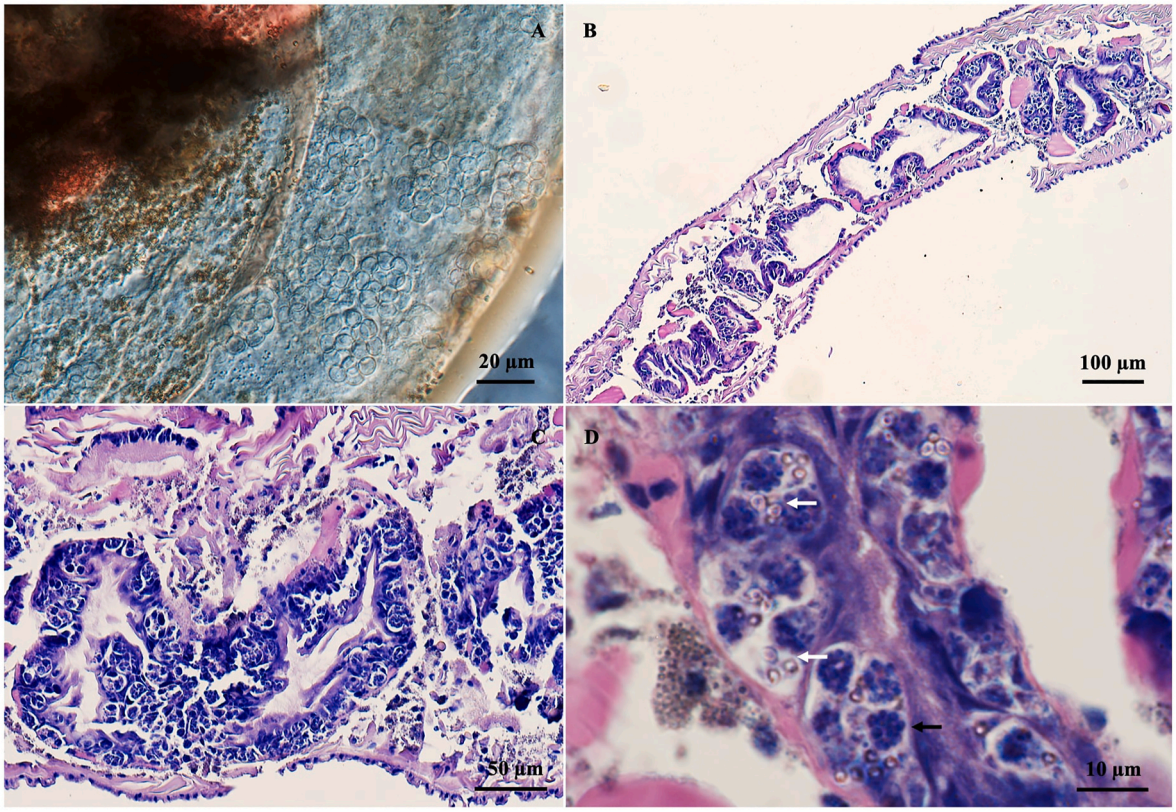

Fig. 7. Pansporocysts of new type of aurantiactinomyxon type 2. A) Higher magnification of the infected oligochaete showing numerous pansporocysts. B-C) Semithin sections showing heavily infected *Tubifex tubifex* with pansporocysts at various stages of development in the intestinal epithelium. D) Mature spores with polar capsules (white arrow) and secondary cells (black arrow) can be seen.

of two years with more frequent sample collection at biweekly intervals.

The triactinomyxon type described in this study was morphologically similar to triactinomyxon type 2 (Székely et al., 2014), but differed morphometrically. Remarkably, the length and width of the triactinomyxon type identified in this study were distinct from all known triactinomyxon types described in the literature. The life cycles of myxosporeans appears to maintain a correlation between actinospore morphotypes and myxosporean genera in both marine and freshwater environments. For example, the tetractinomyxon morphotype has been associated to the life cycles of species such as *Ellipsomyxa* (Køie et al., 2004; Rangel et al., 2009), *Gadimyxa* (Køie et al., 2007), *Parvicapsula* (Køie et al., 2013), *Sigmomyxa* (Karlsbakk and Køie, 2012), and *Ceratomyxa* (Køie et al., 2008) in the marine environment. Similarly, in freshwater environments, the triactinomyxon morphotype is mainly associated with the life cycles of *Myxobolus* species (Yokoyama, 2003). However, there are a few *Myxobolus* species such as *Myxobolus cultus* (Yokoyama et al., 1995), *Myxobolus dispar* (Molnár et al., 1999; Holzer et al., 2004) and *Myxobolus lentisuturalis* (Caffara et al., 2009), that have been recorded to have raabeia type actinospore stages. The phylogenetic tree and genetic distance analysis support this observation, as the triactinomyxon identified in this study shows close genetic similarity to *Myxobolus* spp. and is grouped within a clade primarily containing gill-infecting *Myxobolus* spp. from cyprinid fish (Fig. 8). The triactinomyxon in this study shares a genetic affinity with *M. diversicapsularis*, which parasitizes the gill lamellae of *Rutilus rutilus*. This is significant because *M. diversicapsularis* has a known life cycle involving triactinomyxon actinospores (Eszterbauer et al., 2015), highlighting the possibility that the identified triactinomyxon type in the present study could also complete its life cycle in cyprinid hosts, developing into a *Myxobolus* species in the gills of fish. So far, life cycles involving triactinomyxon types have been described for *M. drjagini* (El-Mansy and Molnár, 1997a), *M. hungaricus* (El-Mansy and Molnár, 1997b), *M. portucalensis* (El-Mansy et al., 1998c), *M. bramae* (Eszterbauer et al., 2000), *M. pseudodispar* (Székely et al., 1999, 2001), *M. macrocapsularis* (Székely et al., 2002), *M. intimus* (Rácz et al., 2004), *M. rotundus* (Székely et al., 2009), *M. wootteni,* and *M. diversicapsularis* (Molnár et al., 2010), *M. erythrophthalmi*, *M. fundamentalis* and *M. shaharomae* (Székely et al., 2014) in Hungary. Therefore, future work should aim to collect more cyprinids from the same ponds to elucidate the life cycle by identifying the potential myxospore stage of the triactinomyxon type.

The raabeia type described in this study exhibits morphology similar to raabeia type 2 (Borkhanuddin et al., 2014) and minimal morphometric differences from "triactinomyxon 'F'" (Xiao and Desser, 1998). These minimal morphometric variations between the raabeia type identified in this study and "triactinomyxon 'F'" could be explained by their infection of similar oligochaete hosts, specifically *L. hoffmeisteri*. In contrast, raabeia type 2 described by Borkhanddin et al. (2014) exhibits distinct morphometric variations due to the actinospores developing in *Isochaetides michaelseni*. Both the raabeia type from this study and "triactinomyxon 'F'" share key characteristics with the raabeia collective group, which is characterized by an elongated spore body without a style and caudal processes that curve upwards. However, Xiao and Desser (1998) classified "triactinomyxon 'F'" within the triactinomyxon collective group rather than the raabeia collective group, possibly due to confusion or challenges in accurately assigning spore types to these groups in earlier studies. Given that our raabeia type is morphologically similar to the raabeia collective group (lacking a style) and displaying distinct differences from the triactinomyxon collective group. Thus, we have classified our raabeia type within the raabeia collective group. Furthermore, the placement of our raabeia spore within raabeia type 1 (KJ152184) in the phylogenetic tree suggests significant morphological overlap. The phylogenetic analysis performed in this study revealed that the raabeia type described here clusters with "triactinomyxon 'F'" and is

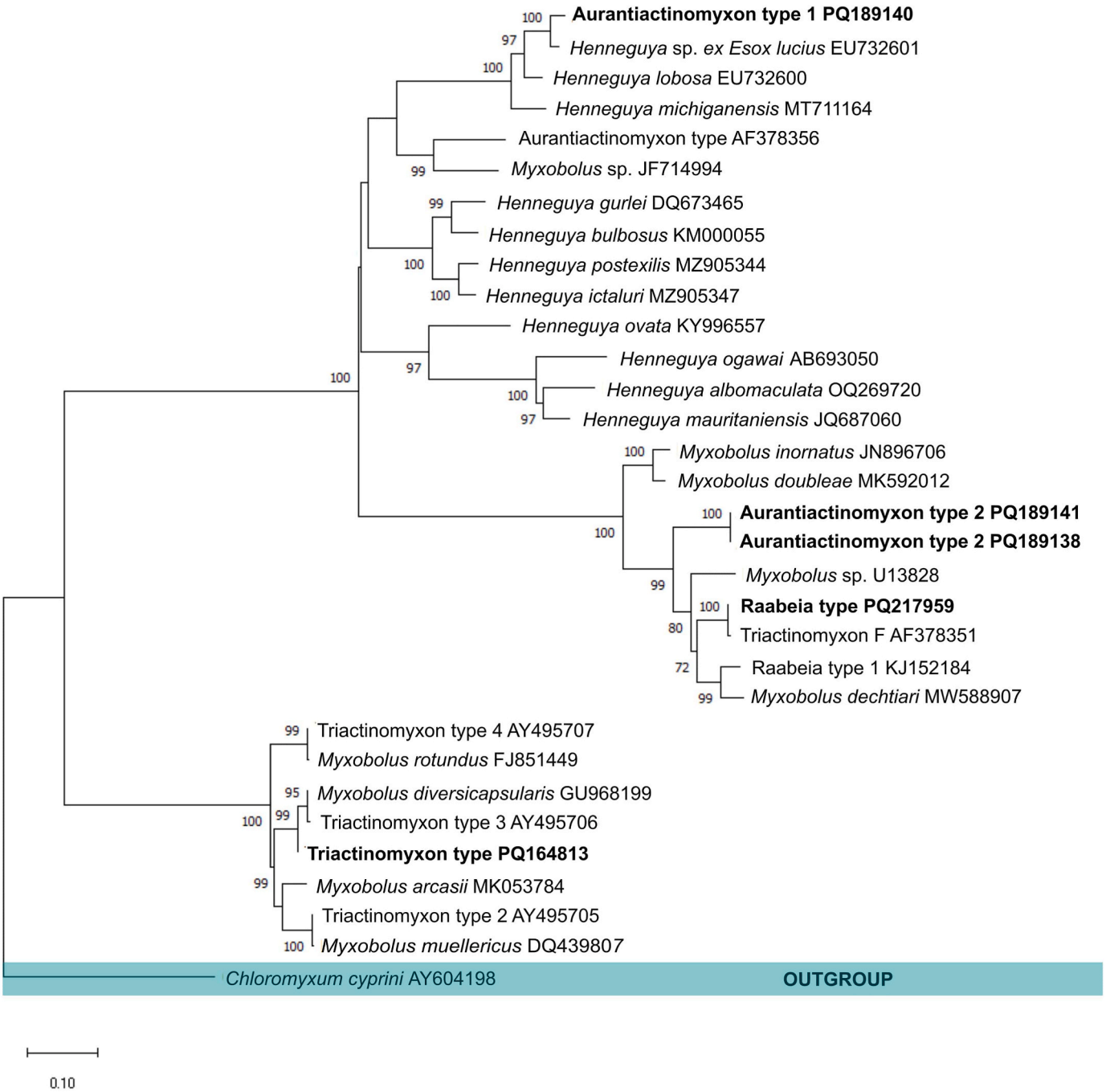

Fig. 8. Maximum likelihood phylogenetic tree based on small subunit 18S ribosomal DNA sequences of the actinosporeans studied and related species. The tree is rooted to the *Chloromyxum cyprini* as the outgroup, with bootstrap support ≥70% indicated at nodes. GenBank accession numbers are given in parentheses, followed by the name of the parasite species. Actinosporean examined in the present study are in bold. The scale bar indicates the number of expected substitutions per site.

closely related to raabeia type 1 and *Myxobolus* spp. infecting the gills of *Lepomis gibbosus* and *Cottus bairdii* (Fig. 8). This suggests that the corresponding myxospore stages of the raabeia type may develop in the gills of perciform or scorpaeniform fishes and have close affinities to the genus *Myxobolus*. However, to the best of our knowledge, the fish farms where the oligochaetes were collected do not contain scorpaeniform fishes. Therefore, future work should focus on collecting more fish from the order Perciformes and thoroughly examining their gills to elucidate the life cycle by identifying the potential myxospore stage of the raabeia type.

Actinospores belonging to the aurantiactinomyxon collective group often present challenges when comparing morphological characteristics, as this approach is unreliable for distinguishing among different aurantiactinomyxon types (Hallett et al., 2002; Eszterbauer et al., 2006; Zhao et al., 2016). In this study, both aurantiactinomyxon type 1 and aurantiactinomyxon type 2 were compared using morphological, morphometric, and molecular analyses. Notable differences were observed between them in all morphological features including the length and width of the caudal processes, spore body diameters, polar capsules diameter, and the number of secondary cells (Table 2). Distinct morphometric variations between the aurantiactinomyxon type 1 and aurantiactinomyxon type 2 could be explained by their infection of different oligochaete hosts: *Ophidonais serpentina* and *Tubifex tubifex*. Four aurantiactinomyxon types have been previously reported within

the genus *Nais*, in *Nais bretscheri* (Bartholomew et al., 1992), *Nais elinguis* (Trouillier et al., 1996), and *Nais* spp. (Grossheider and Korting, 1992; Borkhanuddin et al., 2014; Borzák et al., 2021). However, no myxosporean infections have been reported from *Ophidonais serpentina*. Aurantiactinomyxon types produced by *Nais* spp. as described by Grossheider and Korting (1992), Borkhanuddin et al. (2014), and Borzák et al. (2021), may originated from *Ophidonais serpentina* host; however, the authors did not provide details on the morphology of the hosts, preventing confirmation that the oligochaete host is indeed *Ophidonais serpentina*. This new record suggests that *Ophidonais serpentina* is a previously unrecognized annelid host for myxospores within the family Naididae in freshwater environments and may harbour a greater diversity of these parasites and infections that is currently known. Additionally, ten aurantiactinomyxon types have been reported from *Tubifex tubifex* (El-Matbouli et al., 1992; El-Mansy et al., 1998b; Székely et al., 1998, 2003; Hallett et al., 2002; Özer et al., 2002; Morris and Freeman, 2010). All these ten previously described aurantiactinomyxon types exhibit distinct morphological and morphometric characteristics compared to aurantiatinomyxon type 2 identified in this study. The infection in *Tubifex tubifex* indicates that this oligochaete is suitable host for the development of aurantiactinomyxon.

Molecular studies have demonstrated that aurantiactinomyxon type 1 and aurantiacinomyxon 2 do not share significant genetic similarities, with value of 69.4%. It is also supported by the phylogenetic tree, which shows that aurantiactinomyxon type 1 and aurantiactinomyxon type 2 are placed in separate clades: one associated with *Henneguya* species and the other with *Myxobolus* species. Aurantiactinomyxon type 1 is closely related to *Henneguya* sp. from *Esox lucius* and *Henneguya lobosa*, and it groups within a clade containing gill-infecting *Henneguya* spp. from Esociformes fish (Fig. 8). It suggests that the corresponding myxospore stages of the aurantiactinomyxon type 1 may develop in the gills of fish from order Esociformes and have close affinities to the genus *Henneguya*. To date, only three *Henneguya* spp. namely *H. psorospermica* (Thélohan, 1895), *H. lobosa* (Cohn, 1895), and *H. michiganensis* (Rosser et al., 2021) have been found to infect the gills of fish from the order Esociformes. However, only one of these species has been reported to infect the gills of *Esox lucius* in Hungary (Székely et al., 2018). In addition, aurantiactinomyxon type 2 is closely related to *Myxobolus inornatus* and *Myxobolus doubleae*, and it groups within a clade containing *Myxobolus* spp. from order Perciformes (Fig. 8). This indicates that the corresponding myxospore stages of the aurantiactinomyxon type 2 may develop in fish from the order Perciformes and have close affinities to the genus *Myxobolus*. Therefore, future work should concentrate on collecting *Esox lucius* and thoroughly examining the gills, as well as collecting other fish species from the order Perciformes to elucidate the life cycle by identifying the potential myxospore stages of aurantiactinomyxon type 1 and aurantiactinomyxon type 2.

Overall, the phylogenetic tree and genetic distance analysis in our study supported that myxozoan species tend to cluster based on host species and their tissue specificity. Specifically, the triactinomyxon type, raabeia type, aurantiactinomyxon type 1 and aurantiactinomyxon type 2 of this study are primarily grouped within a gill-infecting clade, targeting fish from Cypriniformes, Esociformes and Perciformes (host specificity). This finding is consistent with previous studies that showed myxosporean parasites clustering based on their host species and infection sites (Fiala and Bartosová, 2010; Liu et al., 2011), which suggests a possible co-evolution between the parasites and their hosts, where parasites adapt to specific hosts and tissues, leading to speciation events. Furthermore, gills serve as a common infection site for many myxozoans due to their dense and fine capillary network, thin epithelial barriers, and direct contact with the environment, which facilitate parasite entry and transmission (Lom and Dyková, 2006).

Traditionally, most life cycle studies of myxozoans were based on experimental infections (El-Matbouli and Hoffmann, 1989, 1993; El-Mansy and Molnár, 1997a, b; El-Mansy et al., 1998c; Székely et al., 1999, 2001, 2002, 2009; Eszterbauer et al., 2000; Rácz et al., 2004), that offer several advantages for researchers, including laboratory studies under controlled conditions and manipulation of experimental settings such as temperature, parasite dose, etc. Additionally, it allow for the assessment of the pathogenic potential of various myxozoan species. However, these experimental studies were often laborious, time-consuming, and produced questionable results. The use of molecular tools has provided an alternative approach to identifying the appropriate developmental stages (actinospore-myxospore pairs), leading to more reliable and accurate confirmation of myxozoan life cycles. Molecular analysis has also proven particularly useful in the identification of congeneric myxozoan species with only minor morphological and spore structural differences that were difficult to distinguish using traditional morphological methods alone. According to the latest review by Eszterbauer et al. (2015), the life cycles of 34 myxozoan species have been successfully identified using molecular analysis. Since then, eight more actinospores were matched with myxospores using molecular methods (Rangel et al., 2015, 2017; Zhao et al., 2017; Rocha et al., 2020; Jorge et al., 2022; Tilley et al., 2024). However, in the current study, the actinospores did not match any of the known myxosporean developmental stage sequences available in GenBank, indicating that more myxozoan species are yet to be discovered in the fish farm ecosystems or that some described myxospores have not passed molecular analysis.

In conclusion, four actinospore types were described through both morphological and molecular analyses, collected from three oligochaete host species. Additionally, comprehensive surveys of fish stocks, particularly those belonging to the orders Cypriniformes, Esociformes, and Perciformes in these fish farms are necessary, as they may serve as potential hosts for the four actinospore types described in this study. Remarkably, this survey has documented the occurrence of two oligochaetes species, *Branchiodrilus hortensis* and *Ophidonais serpentina*, in Hungary for the first time, with one of these species serving as a host for aurantiactinomyxon type 1.

Funding sources

This work was supported by the Stipendium Hungaricum Program.

CRediT authorship contribution statement

Nadhirah Syafiqah Suhaimi: Writing – original draft, Visualization, Validation, Software, Methodology, Investigation, Formal analysis, Data curation, Conceptualization. **Boglárka Sellyei:** Writing – review & editing, Validation, Supervision, Software, Methodology, Data curation, Conceptualization. **Zsolt Udvari:** Writing – review & editing, Validation, Resources, Methodology. **Csaba Székely:** Writing – review & editing, Supervision, Resources, Project administration, Methodology, Funding acquisition, Conceptualization. **Gábor Cech:** Writing – review & editing, Validation, Supervision, Software, Methodology, Data curation, Conceptualization.

Declaration of competing interest

Please check the following as appropriate:

- o All authors have participated in (a) conception and design, or analysis and interpretation of the data; (b) drafting the article or revising it critically for important intellectual content; and (c) approval of the final version.
- o This manuscript has not been submitted to, nor is under review at, another journal or other publishing venue.
- o The authors have no affiliation with any organization with a direct or indirect financial interest in the subject matter discussed in the manuscript
- o The following authors have affiliations with organizations with direct or indirect financial interest in the subject matter discussed in the manuscript:

Acknowledgements

We thank the Ráckeve Danube Arm Fishing Association and Mr. Gábor Nagy for granting permission to collect sediment samples in the fish farms. We also thank Ms. Györgyi Pataki for the histological slides and Mr. Yuzwan Mohamad for GIS mapping.

Appendix A. Supplementary data

Supplementary data to this article can be found online at https://doi.org/10.1016/j.ijppaw.2024.100994.

References

Arslan, N., Şahin, Y., 2006. A preliminary study on the identification of the littoral oligochaete (Annelida) and Chironomidae (Diptera) fauna of Lake Kovada, a national park in Turkey. Turk. J. Zool. 30, 67–72.

Atanacković, A., Šporka, F., Marković, V., Slobodnik, J., Zorić, K., Csányi, B., Paunović, M., 2020. Aquatic worm assemblages along the Danube: a homogenization warning. Water 12, 2612. https://doi.org/10.3390/w12092612.

Atanacković, A., Zorić, K., Paunović, M., 2021. Invading Europe: the tropical aquatic worm *Branchiodrilus hortensis* (Stephenson, 1910) (Clitellata, Naididae) extends its range. BioInvasions Rec. 10, 598–604.

Atkinson, S.D., Bartholomew, J.L., 2009. Alternate spore stages of *Myxobilatus gasterostei*, a myxosporean parasite of three-spined sticklebacks (*Gasterosteus aculeatus*) and oligochaetes (*Nais communis*). Parasitol. Res. 104, 1173–1181. https://doi.org/10.1007/s00436-008-1308-6.

Barta, J.R., Martin, D.S., Liberator, P.A., Dashkevicz, M., Anderson, J.W., Feighner, S.D., Elbrecht, A., Perkins-Barrow, A., Jenkins, M.C., Danforth, H.D., Ruff, M.D., Profous-Juchelka, H., 1997. Phylogenetic relationships among eight *Eimeria* species infecting domestic fowl were inferred using complete small subunit ribosomal DNA sequences. J. Parasitol. 83, 262–271. https://doi.org/10.2307/3284453.

Bartholomew, J.L., Fryer, J.L., Rohovec, J.S., 1992. *Ceratomyxa shasta* infections of salmonid fish. In: Proceedings OJI International Symposium Salmonid Diseases. Hokkaido University Press, Sapporo, pp. 267–275.

Bartholomew, J.L., Atkinson, S.D., Hallett, S.L., Lowenstine, L.J., Garner, M.M., Gardiner, C.H., Rideout, B.A., Keel, M.K., Brown, J.D., 2008. Myxozoan parasitism in waterfowl. Int. J. Parasitol. 38, 1199–1207.

Baumgartner, S., Brückmann, J., Theurer, J., 2020. Erstnachweis von *Branchiodrilus hortensis* (Stephenson, 1910) (Oligochaeta, Naididae) in Deutschland. Lauterbornia 87, 122–126.

Borkhanuddin, M.H., 2013. Studies of Fish Parasitic Myxozoans in Lake Balaton, Hungary and in Freshwater and Marine Biotopes in Malaysia. University of Pannonia, Hungary, pp. 1–107. PhD thesis.

Borkhanuddin, M.H., Cech, G., Molnár, K., Németh, S., Székely, C., 2014. Description of raabeia, synactinomyxon and neoactinomyxum developing stages of myxosporeans (myxozoa) infecting *Isochaetides michaelseni* lastočkin (Tubificidae) in Lake Balaton and kis-balaton water Reservoir, Hungary. Syst. Parasitol. 88, 245–259. https://doi.org/10.1007/s11230-014-9496-1.

Borzák, R., Borkhanuddin, M.H., Cech, G., Molnár, K., Hallett, S.L., Székely, C., 2021. New data on *Thelohanellus nikolskii* Achmerov, 1955 (Myxosporea, Myxobolidae) a parasite of the common carp (*Cyprinus carpio*, L.): the actinospore stage, intrapiscine tissue preference and molecular sequence. Int. J. Parasitol. Parasites Wildl. 15, 112–119. https://doi.org/10.1016/j.ijppaw.2021.04.004.

Brinkhurst, R.O., Jamieson, B.G.M., 1971. Aquatic Oligochaeta of the World. Oliver & Boyd, Edinburg, p. 860.

Caffara, M., Raimondi, E., Florio, D., Marcer, F., Quaglio, F., Fioravanti, M.L., 2009. The life cycle of *Myxobolus lentisuturalis* (Myxozoa: myxobolidae), from goldfish (*Carassius auratus auratus*), involves a raabeia-type actinospore. Folia Parasitol. 56, 6–12.

Cekanovskaja, O.V., 1962. Vodnye malostetinkovye cervi fauny SSSR. Opredeliteli Po Faune SSSR. Izdatelstvo Akademii Nauk SSSR, Moskva, p. 409.

Claparède, E., 1862. Recherches sur les oligochètes. Mem. Soc. Phys. Hist. Nat. Geneve 16, 217–291.

Cohn, L., 1895. Über die Myxosporidien von *Esox lucius* and *Perca fluviatilis*. Inagural Dissertation, Albertus Universität, Königsberg 48.

Diamant, A., Whipps, C.M., Kent, M.L., 2004. A new species of *Sphaeromyxa* (Myxosporea: sphaeromyxina: Sphaeromyxidae) in devil firefish, *Pterois miles* (Scorpaenidae), from the northern Red Sea: morphology, ultrastructure, and phylogeny. J. Parasitol. 90, 1434–1442. https://doi.org/10.1645/GE-336R.

Dyková, I., Tyml, T., Fiala, I., Lom, J., 2007. New data on *Soricimyxum fegati* (Myxozoa) including analysis of its phylogenetic position inferred from the SSU rRNA gene sequence. Folia Parasitol. 54, 272. https://doi.org/10.14411/fp.2007.035.

El-Mansy, A., Molnár, K., 1997a. Extrapiscine development of *Myxobolus drjagini* Akhmerov, 1954 (Myxosporea: myxobolidae) in oligochaete alternate hosts. Acta Vet. Hung. 45, 427–438.

El-Mansy, A., Molnár, K., 1997b. Development of *Myxobolus hungaricus* (Myxosporea: myxobolidae) in oligochaete alternate hosts. Dis. Aquat. Org. 31, 227–232. https://doi.org/10.3354/dao031227.

El-Mansy, A., Székely, C., Molnár, K., 1998a. Studies on the occurrence of actinosporean stages of myxosporeans in Lake Balaton, Hungary, with the description of triactinomyxon, raabeia and aurantiactinomyxon types. Acta Vet. Hung. 46, 437–450.

El-Mansy, A., Székely, C., Molnár, K., 1998b. Studies on the occurrence of actinosporean stages of fish myxosporeans in a fish farm of Hungary, with the description of triactinomyxon, raabeia, aurantiactinomyxon and neoactinomyxon types. Acta Vet. Hung. 46, 259–284.

El-Mansy, A., Molnár, K., Székely, C., 1998c. Development of *Myxobolus portucalensis* saraiva & Molnár, 1990 (myxosporea: myxobolidae) in the oligochaete *Tubifex tubifex* (müller). Syst. Parasitol. 41, 95–103.

El-Matbouli, M., Hoffmann, R.W., 1989. Experimental transmission of two *Myxobolus* spp. developing by sporogeny via tubificid worms. Parasitol. Res. 75, 461–464.

El-Matbouli, M., Fischer-Scherl, T., Hoffmann, R.W., 1992. Transmission of *Hoferellus carassii* Achmerov, 1960 to goldfish *Carassius auratus* via an aquatic oligochaete. Bull. Eur. Assoc. Fish Pathol. 12, 54–56.

El-Matbouli, M., Hoffmann, R.W., 1993. *Myxobolus carassii* Klokaceva, 1914 also requires an aquatic oligochaete, *Tubifex tubifex* as intermediate host in its life cycle. Bull. Eur. Assoc. Fish Pathol. 13, 189–192.

Eszterbauer, E., Székely, C., Molnár, K., Baska, F., 2000. Development of *Myxobolus bramae* (Myxosporea: myxobolidae) in an oligochaete alternate host, *Tubifex tubifex*. J. Fish. Dis. 23, 19–25. https://doi.org/10.1046/j.1365-2761.2000.00202.x.

Eszterbauer, E., Székely, C., 2004. Molecular phylogeny of the kidney-parasitic *Sphaerospora renicola* from common carp (*Cyprinus carpio*) and *Sphaerospora* sp. from goldfish (*Carassius auratus auratus*). Acta Vet. Hung. 52, 469–478.

Eszterbauer, E., Marton, S., Rácz, O.Z., Letenyei, M., Molnár, K., 2006. Morphological and genetic differences among actinosporean stages of fish-parasitic myxosporeans (Myxozoa): difficulties of species identification. Syst. Parasitol. 65, 97–114. https://doi.org/10.1007/s11230-006-9041-y.

Eszterbauer, E., Sipos, D., Forró, B., Holzer, A.S., 2013. Molecular characterization of *Sphaerospora molnari* (Myxozoa), the agent of gill sphaerosporosis in common carp *Cyprinus carpio*. Dis. Aquat. Org. 104, 59–67. https://doi.org/10.3354/dao02584.

Eszterbauer, E., Atkinson, S., Diamant, A., Morris, D., El-Matbouli, M., Hartikainen, H., 2015. Myxozoan life cycles: practical approaches and insights. In: Myxozoan Evolution, Ecology and Development. Springer, London, UK, pp. 175–198. https://doi.org/10.1007/978-3-319-14753-6_10.

EUMOFA, 2023. The E.U. Fish Market 2023 Edition. Publications Office of the European Union, Luxembourg. https://eumofa.eu/documents/20124/35668/EFM2023_EN.pdf/95612366-79d2-a4d1-218b-8089c8e7508c?t=1699541180521c. (Accessed 2 July 2024).

Fiala, I., 2006. The phylogeny of Myxosporea (Myxozoa) based on small subunit ribosomal RNA gene analysis. Int. J. Parasitol. 36, 1521–1534.

Fiala, I., Bartosová, P., 2010. History of myxozoan character evolution on the backbone of a phylogeny inferred from ribosomal RNA genes. Parasitology 137, 456–471.

Forró, B., Eszterbauer, E., 2016. Correlation between host specificity and genetic diversity for the muscle-dwelling fish parasite *Myxobolus pseudodispar*: examples of myxozoan host-shift? Folia Parasitol. 63, 1. https://doi.org/10.14411/fp.2016.019.

Freeman, M.A., Kristmundsson, A., 2018. Studies of *Myxidium giardi* Cépède, 1906 infections in Icelandic eels identifies a genetically diverse clade of myxosporeans that represents the *Paramyxidium* n. g. (Myxosporea: myxidiidae). Parasites Vectors 11, 551. https://doi.org/10.1186/s13071-018-3087-y.

George, A.D.I., Abowei, J.F.N., Daka, E.R., Jasper, A., 2009. Benthic macro invertebrate fauna and physico-chemical parameters in Okpoka Creek sediments, Niger Delta, Nigeria. Int. J. Anim. Vet. Adv. 1, 59–65.

Grossheider, G., Körting, W., 1992. First evidence that *Hoferellus cyprini* (doflein, 1898) is transmitted by *Nais* sp. Bull. Eur. Ass. Fish Pathol. 12, 17–20. https://www.cabdirect.org/cabdirect/abstract/19940807289.

Hallett, S.L., Diamant, A., 2001. Ultrastructure and small-subunit ribosomal DNA sequence of *Henneguya lesteri* n. sp. (Myxosporea), a parasite of sand whiting *Sillago analis* (Sillaginidae) from the coast of Queensland, Australia. Dis. Aquat. Org. 46, 197–212. https://doi.org/10.3354/dao046197.

Hallett, S.L., Atkinson, S.D., El-Matbouli, M., 2002. Molecular characterization of two aurantiactinomyxon (Myxozoa) phenotypes reveal one genotype. J. Fish. Dis. 25, 627–631.

Hillis, D.M., Dixon, M.T., 1991. Ribosomal DNA: molecular evolution and phylogenetic inference. Q. Rev. Biol. 66, 411–453. https://doi.org/10.1086/417338.

Holzer, A.S., Sommerville, C., Wootten, R., 2004. Molecular relationships and phylogeny in a community of myxosporeans and actinosporeans based on their 18S rDNA sequences. Int. J. Parasitol. 34, 1099–1111. https://doi.org/10.1016/j.ijpara.2004.06.002.

Janiszewska, J., 1957. Actinomyxidia II. New systematics, sexual cycles, description of new genera and species. Zool. Pol. 8, 3–34.

Jorge, M., Vieira, D.H.M.D., Zago, A.C., Franceschini, L., da Silva, R.J., 2022. *Henneguya polarislonga* n. sp. (Cnidaria: myxosporea) parasitizing *Astyanax lacustris* (Lütken, 1875) with an insight on its life cycle. Parasitol. Int. 91, 102658. https://doi.org/10.1016/j.parint.2022.102658.

Karlsbakk, E., Køie, M., 2012. The marine myxosporean *Sigmomyxa sphaerica* (Thélohan, 1895) gen. n., comb. n. (syn. *Myxidium sphaericum*) from garfish (*Belone belone* (L.)) uses the polychaete *Nereis pelagica* L. as invertebrate host. Parasitol. Res. 110, 211–218. https://doi.org/10.1007/s00436-011-2471-8.

Kearse, M., Moir, R., Wilson, A., Stones-Havas, S., Cheung, M., Sturrock, S., Cheung, M., Sturrock, S., Buxton, S., Cooper, A., Markowitz, S., Duran, C., Thierer, T., Ashton, B., Meintjes, P., Drummond, A., 2012. Geneious basic: an integrated and extendable desktop software platform for the organization and analysis of sequence data. Bioinformatics 28, 1647–1649. https://doi.org/10.1093/bioinformatics/bts199.

Køie, M., Whipps, M., Kent, M.L., 2004. *Ellipsomyxa gobii* (myxozoa: ceratomyxidae) in the common goby *Pomatoschistus microps* (teleostei: gobiidae) uses *nereis* spp. (Annelida: polychaeta) as invertebrate hosts. Folia Parasitol. 51, 14–18.

Køie, M., Karlsbakk, E., Nylund, A., 2007. A new genus *Gadimyxa* with three new species (Myxozoa, Parvicapsulidae) parasitic in marine fish (Gadidae) and the two-host life cycle of *Gadimyxa atlantica* n. sp. J. Parasitol. 93, 1459–1467. https://doi.org/10.1645/GE-1256.1.

Køie, M., Karlsbakk, E., Nylund, A., 2008. The marine herring myxozoan *Ceratomyxa auerbachi* (Myxozoa: ceratomyxidae) uses *Chone infundibuliformis* (Annelida: polychaeta: Sabellidae) as invertebrate host. Folia Parasitol. 55, 100–104.

Køie, M., Karlsbakk, E., Einen, A.C.B., Nylund, A., 2013. A parvicapsulid (Myxozoa) infecting *Sprattus sprattus* and *Clupea harengus* (Clupeidae) in the Northeast Atlantic uses *Hydroides norvegicus* (Serpulidae) as invertebrate host. Folia Parasitol. 60, 149–154. https://doi.org/10.14411/fp.2013.016.

Krno, I., Šporka, F., Matis, D., Tirjaková, E., Halgoš, J., Košel, V., Bulánková, E., Illéšová, D., 1999. Development of Zoobenthos in the Slovak Danube Inundation Area after the Gabčíkovo Hydropower Structures Began Operating. Faculty of Natural Science, Comenius University Bratislava, Slovakia, pp. 233–240.

Krodkiewska, M., Strzelec, M., Spyra, A., 2016. Assessing the diversity of the benthic oligochaete communities in urban and woodland ponds in an industrial landscape (Upper Silesia, southern Poland). Urban Ecosyst. 19, 1197–1211.

Kumar, S., Stecher, G., Li, M., Knyaz, C., Tamura, K., 2018. Mega X: molecular evolutionary genetics analysis across computing platforms. Mol. Biol. Evol. 35, 1547–1549.

Liu, Y., Whipps, C.M., Gu, Z.M., 2011. Phylogeny of *Myxobolus* species (Myxozoa), parasitizing cyprinid fishes in China, based on 18S rDNA sequences. Parasitol. Res. 108, 707–716.

Lom, J., McGeorge, J., Feist, S.W., Morris, D., Adams, A., 1997. Guidelines for the uniform characterization of the actinosporean stages of parasites of the phylum Myxozoa. Dis. Aquat. Org. 30, 1–9. https://doi.org/10.3354/dao030001.

Lom, J., Dyková, I., 2006. Myxozoan genera: definition and notes on taxonomy, life-cycle terminology and pathogenic species. Folia Parasitol. 53, 1–36.

Lowers, J.M., Bartholomew, J.L., 2003. Detection of myxozoan parasites in oligochaetes imported as food for ornamental fish. J. Parasitol. 89, 84–91. https://doi.org/10.1645/0022-3395(2003)089[0084:DOMPIO]2.0.CO;2.

Marques, A., 1984. Contribution á la connaissance des Actinomyxidies: ultrastructure, cycle biologique, systématique. Université des Sciences et Techniques de Languedoc. PhD Thesis 218. Montepellier, France.

Martin, P., Martinsson, S., Wuillot, J., Erseus, C., 2018. Integrative species delimitation and phylogeny of the branchiate worm *Branchiodrilus* (Clitellata, Naididae). Zool. Scripta 47, 727–742. https://doi.org/10.1111/zsc.12316.

Marton, S., Eszterbauer, E., 2011. The development of *Myxobolus pavlovskii* (Myxozoa: myxobolidae) includes an echinactinomyxon-type actinospore. Folia Parasitol. 58, 157.

McGeorge, J., Sommerville, C., Wootten, R., 1997. Studies of actinosporean myxozoan stages parasitic in oligochaetes from the sediments of a hatchery where Atlantic salmon harbour *Sphaerospora truttae* infection. Dis. Aquat. Org. 30, 107–119. https://doi.org/10.3354/dao030107.

Molnár, K., El-Mansy, A., Székely, C., Baska, F., 1999. Development of *Myxobolus dispar* (Myxosporea: myxobolidae) in an oligochaete alternate host, *Tubifex tubifex*. Folia Parasitol. 46, 15–21.

Molnár, K., Marton, S., Székely, C., Eszterbauer, E., 2010. Differentiation of *Myxobolus* spp. (myxozoa: myxobolidae) infecting roach (*Rutilus rutilus*) in Hungary. Parasitol. Res. 107, 1137–1150. https://doi.org/10.1007/s00436-010-1982-z.

Morris, D.J., Freeman, M.A., 2010. Hyperparasitism has wide-ranging implications for studies on the invertebrate phase of myxosporean (Myxozoa) life cycles. Int. J. Parasitol. 40, 357–369. https://doi.org/10.1016/j.ijpara.2009.08.014.

Müller, O.F., 2015. Vermium Terrestrium et Fluviatilium II. Hafniae Lipsiae. Available online. https://www.biodiversitylibrary.org/bibliography/46299. (Accessed 15 July 2024).

Nesemann, H., Sharma, G., Sinha, R.K., 2004. Aquatic Annelida (Polychaeta, Oligochaeta, Hirudinea) of the Ganga River and adjacent water bodies in Patna (India: Bihar), with description of a new leech species (Family Salifidae). Ann. Naturhist. Mus. 105, 139–187.

Okamura, B., Gruhl, A., Reft, A.J., 2015. Cnidarian origins of the myxozoa. In: Okamura, B., Gruhl, A., Bartholomew, J. (Eds.), Myxozoan Evolution, Ecology and Development. Springer, Cham. https://doi.org/10.1007/978-3-319-14753-6_3.

Oumouna, M., Hallett, S., Hoffmann, R., El-Matbouli, M., 2003. Seasonal occurrence of actinosporeans (Myxozoa) and oligochaetes (Annelida) at a trout hatchery in Bavaria, Germany. Parasitol. Res. 89, 170–184.

Özer, A., Wootten, R., Shinn, A.P., 2002. Survey of actinosporean types (Myxozoa) belonging to seven collective groups found in a freshwater salmon farm in Northern Scotland. Folia Parasitol. 49, 189–210.

Palumbi, S., Martin, A., Romano, S., McMillan, W.O., Stice, L., Grabowski, G., 2002. The Simple Fools Guide to PCR. University of Hawaii, Honolulu. Available at: Version 2.0 http://palumbi.stanford.edu/SimpleFoolsMaster.

Prunescu, C.C., Prunescu, P., Pucek, Z., Lom, J., 2007. The first finding of myxosporean development from plasmodia to spores in terrestrial mammals: *Soricimyxum fegati* gen. et sp. n. (Myxozoa) from *Sorex araneus* (Soricomorpha). Folia Parasitol. 54, 159.

Rácz, O.Z., Székely, C., Molnár, K., 2004. Intraoligochaete development of *Myxobolus intimus* (Myxosporea: myxobolidae), a gill myxosporean of the roach (*Rutilus rutilus*). Folia Parasitol. 51, 99–207.

Rácz, O.Z., Eszterbauer, E., Molnár, K., 2005. Hungactinomyxon, a new actinosporean type and collective group (Myxozoa) from *Branchiura sowerbyi* Beddard (Oligochaeta). Syst. Parasitol. 61, 107–113. https://doi.org/10.1007/s11230-005-3136-8.

Rangel, L.F., Santos, M.J., Cech, G., Székely, C., 2009. Morphology, molecular data, and development of *Zschokkella mugilis* (Myxosporea, Bivalvulida) in a polychaete alternate host, *Nereis diversicolor*. J. Parasitol. 95, 561–569. https://doi.org/10.1645/GE-1777.1.

Rangel, L.F., Rocha, S., Castro, R., Severino, R., Casal, G., Azevedo, C., Cavaleiro, F., Santos, M.J., 2015. The life cycle of *Ortholinea auratae* (Myxozoa: ortholineidae) involves an actinospore of the triactinomyxon morphotype infecting a marine oligochaete. Parasitol. Res. 114, 2671–2678. https://doi.org/10.1007/s00436-015-4472-5.

Rangel, L.F., Rocha, S., Casal, G., Castro, R., Severino, R., Azevedo, C., Cavaleiro, F., Santos, M.J., 2017. Life cycle inference and phylogeny of *Ortholinea labracis* n. sp. (Myxosporea: ortholineidae), a parasite of the European seabass *Dicentrarchus labrax* (Teleostei: moronidae), in a Portuguese fish farm. J. Fish. Dis. 40, 243–262. https://doi.org/10.1111/jfd.12508.

Rocha, S., Alves, Ă., Fernandes, P., Antunes, C., Azevedo, C., Casal, G., 2019a. New actinosporean description prompts union of the raabeia and echinactinomyxon collective groups (Cnidaria, Myxozoa). Dis. Aquat. Org. 135, 175–191. https://doi.org/10.3354/dao03389.

Rocha, S., Alves, Â., Antunes, C., Azevedo, C., Casal, G., 2019b. Molecular data infers the involvement of a marine aurantiactinomyxon in the life cycle of the myxosporean parasite *Paramyxidium giardi* (Cnidaria, Myxozoa). Parasitology 46, 1555–1563. https://doi.org/10.1017/S0031182019000866.

Rocha, S., Rangel, L.F., Casal, G., Azevedo, C., Rodrigues, P., Santos, M.J., 2020. Involvement of sphaeractinomyxon in the life cycle of mugiliform-infecting *Myxobolus* (Cnidaria, Myxosporea) reveals high functionality of actinospore morphotype in promoting transmission. Parasitology 147, 1320–1329. https://doi.org/10.1017/S0031182020001043.

Rosser, T.G., Griffin, M.J., Quiniou, S.M., Greenway, T.E., Khoo, L.H., Wise, D.J., Pote, L. M., 2014. Molecular and morphological characterization of myxozoan actinospore types from a commercial catfish pond in the Mississippi Delta. J. Parasitol. 100, 828–839. https://doi.org/10.1645/13-446.1.

Rosser, T.G., Loch, T.P., Faisal, M., Baumgartner, W.A., Griffin, M.J., 2021. *Henneguya michiganensis* n. sp. (Cnidaria: myxosporea) from the gills of muskellunge *Esox masquinongy* mitchill (Esociformes: esocidae). Syst. Parasitol. 98, 119–130. https://doi.org/10.1007/s11230-021-09965-5.

Spencer, D.R., Wisseman, R.E., 1993. Some new records of Naididae and Tubificidae (Annelida: Oligochaeta) from Washington. Great. Basin. Nat 395–401.

Šporka, F., 2009. First record of the neozoan species *Branchiodrilus hortensis* (Stephenson, 1910)(Oligochaeta, Naididae) from Slovakia. Lauterbornia 67, 145–149.

Suhaimi, N.S., Colunga-Ramírez, G., Sellyei, B., Cech, G., Molnár, K., Székely, C., 2023. The first detection of *Myxobolus lentisuturalis* Dyková, Fiala et Nie, 2002, a highly pathogenic muscle-infecting parasite of gibel carp (*Carassius auratus gibelio* Berg, 1932) in Hungary. J. Fish. Dis. 46, 1367–1376. https://doi.org/10.1111/jfd.13855.

Székely, C., El-Mansy, A., Molnar, K., Baska, F., 1998. Development of *Thelohanellus hovorkai* and *Thelohanellus nikolskii* (Myxosporea: myxozoa) in oligochaete alternate hosts. Fish Pathol. 33, 107–114. https://doi.org/10.3147/jsfp.33.107.

Székely, C., Molnár, K., Eszterbauer, E., Baska, F., 1999. Experimental detection of the actinospores of *Myxobolus pseudodispar* (Myxosporea: myxobolidae) in oligochaete alternate hosts. Dis. Aquat. Org. 38, 219–224. https://doi.org/10.3354/dao038219.

Székely, C., Molnár, K., Rácz, O., 2001. Complete developmental cycle of *Myxobolus pseudodispar* (gorbunova) (myxosporea: myxobolidae). J. Fish. Dis. 21, 461–468. https://doi.org/10.1046/j.1365-2761.2001.00324.x.

Székely, C., Rácz, O., Molnár, K., Eszterbauer, E., 2002. Development of *Myxobolus macrocapsularis* (Myxosporea: myxobolidae) in an oligochaete alternate host, *Tubifex tubifex*. Dis. Aquat. Org. 48, 117–123. https://doi.org/10.3354/dao048117.

Székely, C., Yokoyama, H., Urawa, S., Timm, T., Ogawa, K., 2003. Description of two new actinosporean types from a brook of fuji mountain, honshu, and from chitose river, hokkaido, Japan. Dis. Aquat. Org. 53, 127–132. https://doi.org/10.3354/dao053127.

Székely, C., Eiras, J.C., Eszterbauer, E., 2005. Description of a new synactinomyxon type from the River Sousa, Portugal. Dis. Aquat. Org. 66, 9–14. https://doi.org/10.3354/dao066009.

Székely, C., Hallett, S.L., Atkinson, S.D., Molnár, K., 2009. Complete life cycle of *Myxobolus rotundus* (Myxosporea: myxobolidae), a gill myxozoan of common bream *Abramis brama*. Dis. Aquat. Org. 85, 147–155. https://doi.org/10.3354/dao02068.

Székely, C., Borkhanuddin, M.H., Cech, G., Kelemen, O., Molnár, K., 2014. Life cycles of three *Myxobolus* spp. from cyprinid fishes of Lake Balaton, Hungary involve triactinomyxon-type actinospores. Parasitol. Res. 113, 2817–2825. https://doi.org/10.1007/s00436-014-3942-5.

Székely, C., Borzák, R., Molnár, K., 2018. Description of *Henneguya jaczoi* sp. n. (Myxosporea, Myxobolidae) from *Perca fluviatilis* (l.) (Pisces, Percidae) with some remarks on the systematics of *Henneguya* spp. of European fishes. Acta Vet. Hung. 66, 426–443.

Thélohan, P., 1895. Recherches sur les Myxosporidies. Bull. Sci. Fr. Belg. 26, 100–394.

Thompson, J.D., Higgins, D.G., Gibson, T.J., 1994. Clustal W: improving the sensitivity of progressive multiple sequence alignment through sequence weighting, position-specific gap penalties and weight matrix choice. Nucleic Acids Res. 22, 4673–4680. https://doi.org/10.1093/nar/22.22.4673.

Tilley, M.F., Barry, D., Hanington, P.C., Goater, C.P., 2024. Description, life cycle, and development of the myxozoan *Myxobolus rasmusseni* n. sp. in fathead minnows, *Pimephales promelas*: a possible emerging pathogen in southern Alberta, Canada. Int. J. Parasitol. Parasites Wildl. 100944. https://doi.org/10.1016/j.ijppaw.2024.100944.

Timm, T., 2009. A guide to the freshwater Oligochaeta and polychaeta of northern and central Europe. Lauterbornia 66, 1–235.

Trouillier, A., El-Matbouli, M., Hoffmann, R.W., 1996. A new look at the life-cycle of *Hoferellus carassii* in the goldfish (*Carassius auratus auratus*) and its relation to kidney. Folia Parasitol. 43, 173–187.

van Haaren, T., Soes, M., Munts, R., 2005. *Branchiodrilus hortensis*, een nieuwe exotische borstelworm in Nederland (Annelida: Oligochaeta). Nederl. Faun. Meded. 22, 17–21.

van Haaren, T., Soors, J., 2013. Aquatic Oligochaetes of The Netherlands and Belgium. KNNV Publishing, The Netherlands, p. 302. https://doi.org/10.1163/9789004278097.

Xiao, C., Desser, S.S., 1998. Actinosporean stages of myxozoan parasites of oligochaetes from Lake Sasajewun, Algonquin Park, Ontario: new forms of triactinomyxon and raabeia. J. Parasitol. 998–1009. https://doi.org/10.2307/3284634.

Yokoyama, H., Ogawa, K., Wakabayashi, H., 1995. *Myxobolus cultus* n. sp. (Myxosporea: myxobolidae) in the goldfish *Carassius auratus* transformed from the actinosporean stage in the oligochaete *Branchiura sowerbyi*. J. Parasitol. 81, 446–451. https://doi.org/10.2307/3283830.

Yokoyama, H., 2003. A review: gaps in our knowledge on myxozoan parasites of fishes. Fish Pathol. 38, 125–136.

Yu, J., Tingting, Z., Hongzhu, W., Yongde, C., 2022. First record of *Ophidonais serpentina* (müller, 1773) (Oligochaeta: Naididae) in China: the occurrence or absence of needles are intraspecific differences. Diversity 14, 265. https://doi.org/10.3390/d14040265.

Zhao, D., Borkhanuddin, M.H., Wang, W., Liu, Y., Cech, G., Zhai, Y., Székely, C., 2016. The life cycle of *Thelohanellus kitauei* (Myxozoa: myxosporea) infecting common carp (*Cyprinus carpio*) involves aurantiactinomyxon in *Branchiura sowerbyi*. Parasitol. Res. 115, 4317–4325. https://doi.org/10.1007/s00436-016-5215-y.

Zhao, D.D., Zhai, Y.H., Liu, Y., Wang, S.J., Gu, Z.M., 2017. Involvement of aurantiactinomyxon in the life cycle of *Thelohanellus testudineus* (Cnidaria: myxosporea) from allogynogenetic gibel carp *Carassius auratus gibelio*, with morphological, ultrastructural, and molecular analysis. Parasitol. Res. 116, 2449–2456. https://doi.org/10.1007/s00436-017-5547-2.